



HAL
open science

[4Fe-4S] cluster trafficking mediated by Arabidopsis mitochondrial ISCA and NFU proteins

Tamanna Azam, Jonathan Przybyla-Toscano, Florence Vignols, Jérémy Couturier, Nicolas Rouhier, Michael K. Johnson

► To cite this version:

Tamanna Azam, Jonathan Przybyla-Toscano, Florence Vignols, Jérémy Couturier, Nicolas Rouhier, et al.. [4Fe-4S] cluster trafficking mediated by Arabidopsis mitochondrial ISCA and NFU proteins. Journal of Biological Chemistry, 2020, 295 (52), pp.18367-18378. 10.1074/jbc.RA120.015726 . hal-03052839

HAL Id: hal-03052839

<https://hal.science/hal-03052839>

Submitted on 11 Dec 2020

HAL is a multi-disciplinary open access archive for the deposit and dissemination of scientific research documents, whether they are published or not. The documents may come from teaching and research institutions in France or abroad, or from public or private research centers.

L'archive ouverte pluridisciplinaire **HAL**, est destinée au dépôt et à la diffusion de documents scientifiques de niveau recherche, publiés ou non, émanant des établissements d'enseignement et de recherche français ou étrangers, des laboratoires publics ou privés.

[4Fe-4S] cluster trafficking mediated by Arabidopsis mitochondrial ISCA and NFU proteins

Tamanna Azam^{1,†}, Jonathan Przybyla-Toscano^{2,†}, Florence Vignols³, Jérémy Couturier², Nicolas Rouhier², and Michael K. Johnson^{1,*}

¹ Department of Chemistry and Center for Metalloenzyme Studies, University of Georgia, Athens, Georgia, 30602, USA

² Université de Lorraine, INRAE, IAM, F-54000 Nancy, France

³ BPMP, Université de Montpellier, CNRS, INRAE, SupAgro, Montpellier, France

Running title: *Fe-S cluster trafficking with plant ISCA and NFU proteins*

[†]equal contribution

*To whom correspondence should be addressed: Department of Chemistry, University of Georgia, Athens, Georgia, 30602, USA

Email: mkj@uga.edu, Tel.: 706-542-9378; Fax: 706-542-9454

Keywords: mitochondria, iron-sulfur protein, *Arabidopsis thaliana*, protein-protein interaction, circular dichroism, Raman spectroscopy, iron-sulfur cluster trafficking, ISCA proteins, NFU proteins

Abstract

Numerous iron-sulfur (Fe-S) proteins with diverse functions are present in the matrix and respiratory chain complexes of mitochondria. Although [4Fe-4S] clusters are the most common type of Fe-S cluster in mitochondria, the molecular mechanism of [4Fe-4S] cluster assembly and insertion into target proteins by the mitochondrial ISC maturation system is not well understood. Here we report a detailed characterization of two late-acting Fe-S cluster carrier proteins from *Arabidopsis thaliana*, NFU4 and NFU5. Yeast two-hybrid and bimolecular fluorescence complementation studies demonstrated interaction of both the NFU4 and NFU5 proteins with the ISCA class of Fe-S carrier proteins. Recombinant NFU4 and NFU5 were purified as apo-proteins after expression in *Escherichia coli*. *In vitro* Fe-S cluster reconstitution led to the insertion of one [4Fe-4S]²⁺ cluster per homodimer as determined by UV-visible absorption/CD, resonance Raman and EPR spectroscopy, and analytical studies. Cluster transfer reactions, monitored by UV-visible absorption and CD spectroscopy, showed that a [4Fe-4S]²⁺ cluster-bound ISCA1a/2 heterodimer is effective in transferring [4Fe-4S]²⁺ clusters to both NFU4 and NFU5 with negligible back reaction. In addition, [4Fe-4S]²⁺ cluster-bound ISCA1a/2, NFU4 and NFU5 were all found to be effective

[4Fe-4S]²⁺ cluster donors for maturation of the mitochondrial apo-aconitase 2 as assessed by enzyme activity measurements. The results demonstrate rapid, unidirectional and quantitative [4Fe-4S]²⁺ cluster transfer from ISCA1a/2 to NFU4 or NFU5 that further delineates their respective positions in the plant ISC machinery and their contributions to the maturation of client [4Fe-4S] cluster-containing proteins.

Iron-sulfur (Fe-S) clusters are protein cofactors that carry out crucial roles in diverse biological processes (1). In plants, these cofactors are present in proteins involved in photosynthesis, nitrogen and sulfur assimilation, respiration, and vitamin, DNA and amino acid metabolism (2,3). The most represented forms are the [4Fe-4S] and [2Fe-2S] clusters with a few proteins incorporating cubane-type [3Fe-4S] clusters. Fe-S cluster biosynthesis and incorporation into client proteins is a regulated process implicating several dedicated assembly machineries, each involving multiple proteins. In plants, three machineries with a different subcellular distribution are present (2,4). While the plastidial sulfur utilization (SUF) machinery operates independently, the cytosolic iron-sulfur protein assembly (CIA) machinery, required for both cytosolic and nuclear Fe-S proteins, depends on the mitochondrial iron-sulfur cluster (ISC) assembly machinery.

The molecular mechanisms for Fe-S cluster assembly are globally similar for each machinery even though the proteins involved may belong to different classes. As an example, the maturation of mitochondrial Fe-S proteins involves the orchestrated action of *ca* 20 proteins and can be divided into several sequential steps (5). The initial steps correspond to the assembly of a [2Fe-2S]²⁺ cluster on the Isu/ISCU/ISU scaffold protein. This *de novo* assembly involves a protein complex formed by the cysteine desulfurase Nfs1/NFS1 and two associated proteins, Isd11/ISD11 and Acp1/ACPI, which together supply the required sulfur atoms by catalyzing cysteine desulfuration (6-9). An additional protein, frataxin (Yfh1/FH/FXN), is proposed to coordinate Fe²⁺ ion entry in the complex and to enhance the persulfide transfer reaction from NFS1 to U-type scaffold proteins (10-13). A ferredoxin (Yah1/FDX) supplies the additional electrons required to reduce the persulfide to sulfide (13,14). After assembly, the ISCU-bound [2Fe-2S]²⁺ cluster is conveyed and transferred using a chaperone/co-chaperone system to target the Fe-S cluster ligating subunits of complex I and specific LYR motif-containing proteins such as SDHB, the Fe-S cluster binding subunit of complex II and LYRM7, an assembly factor for respiratory chain complex III as observed with human proteins (15). Another target for the holo-ISCU-chaperone/co-chaperone complex is the class II/monothiol glutaredoxin (GRX), namely Grx5 in yeast, GLRX5 in human or GRXS15 in plants (16,17). Grx5, which is the first acting Fe-S cluster transfer/carrier protein in yeast, can directly deliver [2Fe-2S] clusters to acceptor proteins, the identity of which remains to be determined. In addition, yeast Grx5 appears to be the last ISC protein connected to the CIA machinery (16,18). Unlike in yeast, *Arabidopsis thaliana* (*Arabidopsis*) *grxs15* mutant lines are lethal indicating that it plays an essential, possibly different, role (19).

The biosynthesis of [4Fe-4S] clusters requires additional steps and another set of cluster-transfer proteins, belonging to the A-type carrier (ATC), NFU and MRP/NTPase protein classes. They are named Isa1/2 and ISCA1a/1b/2, and Nfu1 and NFU4/5, in *Saccharomyces cerevisiae* and *Arabidopsis*, respectively. The *Arabidopsis* P-loop NTPase member, INDH, is not found in *S. cerevisiae* as it is specific to the maturation of the respiratory

complex I and is also referred to as Ind1 in *Yarrowia lipolytica* or NUBPL in human (20,21). In addition, two other types of maturation factors participate to these late assembly steps, namely Bol1/Bol3 and Iba57 in yeast or BOLA4 and IBA57.1 in *Arabidopsis*. Their precise roles are unclear so far, but BOLAs form complexes with GRXs and IBA57s with ISCAAs (22,23). *In vitro* studies using mammalian GLRX5 and ISCAAs have suggested that the [2Fe-2S] to [4Fe-4S] cluster interconversion occurs during the Fe-S cluster transfer between the glutaredoxin and an ISCA1/2 heterodimer (24,25). [4Fe-4S] cluster assembly or release from ISCA heterodimers may be facilitated by the BOLA and IBA57 maturation factors (26,27). This conclusion is strengthened by the observation that in yeast and human, only [4Fe-4S] proteins are affected in *isa1/isca1*, *isa2/isca2* and *iba57* mutants or cell lines (23,28-30). So far, it has been demonstrated that INDH is connected to complex I of the respiratory chain, but the precise role and Fe-S cluster donor of INDH/Ind1/NUBPL remains to be determined (20,21,31,32). The deletion of the unique mitochondrial Nfu1/NFU1 partially affects aconitase, lipoic acid synthase, and succinate dehydrogenase activities, indicating a non-essential role for Nfu1 as a [4Fe-4S]²⁺ cluster donor protein (33-35). Based on the specific or milder molecular phenotypes of the *nfu1* and *nubpl* mutants in yeast or human, it is assumed that these two types of transfer proteins act downstream ATC proteins.

All representatives of the NFU family of proteins share a common NFU domain containing two conserved cysteines in a CXXC motif, that binds an Fe-S cluster at the homodimer subunit interface. It can also be associated to an additional domain of variable nature, thus conferring a large diversity of structural organisation among NFU proteins (36). There are five NFU proteins in *Arabidopsis* divided into two classes. NFU1/2/3 proteins are located in chloroplasts whereas NFU4/5 are proposed to be located in the mitochondrial matrix (37). Plastidial NFU isoforms have an additional C-terminal NFU domain that does not have the Fe-S cluster-ligating cysteines, whereas NFU4/5 have an additional N-terminal domain of unknown function in the same region as found in mitochondrial Nfu1/NFU1 proteins from yeast and human. It is assumed that these extra

domains are involved in targeting specific acceptor proteins, as was documented for the additional ATC domain present in *E. coli* NfuA (36). So far, only plastidial-located NFUs have been characterized in plants. It was demonstrated that NFU2 and very likely NFU3 are required for the maturation of numerous [2Fe-2S] and [4Fe-4S]-containing proteins in plants, including photosystem I subunits and a dihydroxyacid dehydratase involved in branched chain amino acid synthesis (38-41). The importance of these proteins is pointed out by the lethality of an *nfu2 nfu3* mutant in Arabidopsis (40). In contrast, NFU1 is dispensable, at least in standard growth conditions, and solely able to assemble and deliver [4Fe-4S] clusters (40,42). The physiological role of the mitochondrial NFU4/5 isoforms has never been investigated *in planta* so far. However, both NFU4 and NFU5 are able to rescue the growth and biochemical phenotypes of the yeast *nfu1Δ* and *nfu1Δisu1Δ* strains, suggesting that plant orthologs perform functions similar to yeast Nfu1 and interact with the physiological partners of yeast Nfu1 (37,43).

In the present study, we combined complementary *in vivo* and *in vitro* approaches to investigate the properties and interactions of Arabidopsis NFU4/5 proteins. The results demonstrate that NFU4 and NFU5 only bind [4Fe-4S] clusters, as is the case for the yeast and human mitochondrial counterparts. Among other late-acting ISC components, NFU4 and NFU5 interact with ISCA1 proteins and we further showed that an ISCA1a/2 heterodimer is a competent Fe-S cluster donor for the mitochondrial NFU proteins in Arabidopsis and that [4Fe-4S]²⁺ cluster-bound ISCA1a/2, NFU4, and NFU5 are all competent for the maturation of mitochondrial apo-aconitase 2 (ACO2). This work clarifies the position of NFU4/5 proteins in the plant mitochondrial ISC machinery, acting directly downstream of ISCA proteins.

Results

What are the NFU4/5 partners among the ISC components?

In order to identify the partners of mitochondrial NFU proteins among ISC components, we tested whether NFU4 and NFU5 physically interacted with ISC components involved in the late steps, starting

from GRXS15, using binary yeast two-hybrid (Y2H). Only the co-expression of NFU4 or NFU5 with ISCA1a or ISCA1b allowed yeast cell growth in absence of histidine, indicating an interaction between these transfer proteins (Fig. 1A). These interactions were only detectable when NFU4/5 are fused to the DNA binding domain of Gal4. To determine whether both domains of NFU4/5 proteins are necessary for interaction and potentially to assign a role to the additional N-terminal domain, both NFU4/NFU5 domains have been separately expressed in fusion with the Gal4-DNA binding domain and tested with ISCA1a/b, as interactions were only observed with this combination using mature proteins. The N-terminal domain comprised amino acids 80-168 for NFU4 and 75-163 for NFU5 whereas the C-terminal NFU domain harboring the conserved CXXC motif retained amino acids 187-283 for NFU4 and 182-275 for NFU5. Only yeast cells co-expressing ISCA1a/b and the NFU domain of NFU4 or NFU5 grew on medium lacking histidine indicating that this domain is mostly responsible for these interactions (Fig. 1B).

To validate the interaction between NFU4 or NFU5 and ISCA proteins in a plant-based reporter system, bimolecular fluorescence complementation (BiFC) experiments were performed in Arabidopsis protoplasts. A reconstituted YFP fluorescence signal co-localizing with the mitochondrial marker was observed when NFU4 or NFU5 were co-expressed with ISCA1a, ISCA1b in accord with Y2H results, but also with ISCA2 (Fig. 2 and Fig. S1). We have two possible explanations for the divergence of the results obtained by Y2H and BiFC for ISCA2. Either there is indeed a direct interaction between NFU4/5 and ISCA2 that cannot be detected by Y2H or the BiFC signal is due to the presence of ISCA1a/b, which allows forming a ternary complex in plant cells. Altogether, these results indicate that both NFU4 and NFU5 proteins are able to form a stable complex with ISCA1s (at least with ISCA1a) and that these interactions occur in plant mitochondria.

Nature and properties of cluster-bound forms of At NFU4 and NFU5

The nature of Fe-S clusters assembled on NFU4 and NFU5 was determined through spectroscopic and analytical studies of reconstituted samples. Aerobically purified

NFU4 and NFU5 have no visible absorption, indicating that they were purified as apo-proteins (Fig. 3). Anaerobic cysteine desulfurase-mediated cluster reconstitution experiments were conducted in the presence of DTT to address the ability of NFU4 and NFU5 to incorporate Fe-S clusters. Reconstituted NFU4 and NFU5 eluted from the Q-Sepharose column as a single brown fraction. The UV-visible absorption spectra of reconstituted NFU4 and NFU5 are very similar, comprising broad shoulders centered near 320 and 410 nm which are characteristic of $[4\text{Fe-4S}]^{2+}$ clusters (Fig. 3, blue lines). The UV-visible CD spectra of reconstituted NFU4 and NFU5 are also very similar with intense positive and negative bands at 310 and 350 nm, respectively, and weaker positive bands at 440 and 510 nm. These CD spectra are very similar to the reconstituted $[4\text{Fe-4S}]^{2+}$ cluster-bound form of chloroplast NFU1 (42), but quite different from the reconstituted $[4\text{Fe-4S}]^{2+}$ cluster-bound form of chloroplast NFU2 (38), suggesting at least two distinct classes of plant NFU proteins. The broad shoulder in the absorption spectra centered at 400 nm ($A_{400}/A_{280} = 0.28 \pm 0.02$) with a molar extinction coefficient $\epsilon_{400} = 7.5 \pm 0.5 \text{ mM}^{-1}\text{cm}^{-1}$, based on NFU monomer concentration, is indicative of approximately one $[4\text{Fe-4S}]^{2+}$ cluster per NFU4 and NFU5 dimer, in accordance with the protein and iron analyses indicating $2.2 \pm 0.3 \text{ Fe}$ per NFU4/5 monomer (44-46).

The vibrational properties of the $[4\text{Fe-4S}]^{2+}$ cluster in NFU4 and NFU5 were investigated by low temperature resonance Raman spectroscopy. The resonance Raman spectra of NFU4 and NFU5, shown in Fig. 4A, are uniquely characteristic of a $[4\text{Fe-4S}]^{2+}$ cluster. The spectra are similar in terms of Fe-S stretching frequencies and relative intensities to those reported for all-cysteinylligated $[4\text{Fe-4S}]^{2+}$ clusters in ferredoxins and the nitrogenase Fe protein (Table 1). The $[4\text{Fe-4S}]^{2+}$ clusters in NFU4/5 and the nitrogenase Fe protein are both ligated at the subunit interface via CXXC motifs in each subunit. The Fe-S stretching modes are readily assigned, based on normal mode calculations and $^{34}\text{S}^b/^{32}\text{S}^b$ isotope shifts reported for cubane $[\text{Fe}_4\text{S}_4^b]\text{S}_4^t$ units in ferredoxins and appropriate analog complexes, under idealized T_d symmetry, see Table 1 (45,47,48). The most intense bands in the spectra of NFU4 and NFU5 are the totally symmetric (A_1) breathing modes of the cubane

$[\text{Fe}_4\text{S}_4^b]$ core, which are both observed at 338 cm^{-1} . This is in accord with all cysteinyl ligation (frequency range $333\text{--}339 \text{ cm}^{-1}$), whereas replacement of one ligated cysteine by hydroxide, serinate, or aspartate generally results in higher frequencies (frequency range $340\text{--}343 \text{ cm}^{-1}$) (49).

Reduction of $[4\text{Fe-4S}]^{2+}$ cluster-containing NFU4 and NFU5 by incubation with a 10-fold excess of dithionite for 10 min resulted in complete cluster degradation based on UV-visible absorption and EPR studies. This indicates that the reduced $[4\text{Fe-4S}]^{1+}$ clusters are not stable in NFU4 and NFU5 and are unlikely to be physiologically relevant. This conclusion is supported by the observation of EPR signals indicative of a reduced $[4\text{Fe-4S}]^{1+}$ cluster in samples of reconstituted NFU4 and NFU5 reduced with one reducing equivalent of dithionite and frozen within 3 s in liquid nitrogen (Fig. 4B). Identical, near-axial, fast-relaxing $S = 1/2$ EPR signals with $g_{\parallel} = 2.03$ and $g_{\perp} = 1.93$, maximally accounting for 0.35 spins per NFU dimer, were observed for both NFU4 and NFU5. These resonances were only observable without broadening below 30 K indicating fast relaxation, which is characteristic of $[4\text{Fe-4S}]^{1+}$ clusters. The low $S = 1/2$ spin quantification does not result from mixed spin $[4\text{Fe-4S}]^{1+}$ clusters, since low-field resonances around $g = 5$ indicative of $S = 3/2$ $[4\text{Fe-4S}]^{1+}$ clusters were not observed. Rather, the low spin quantification appears to a consequence of the $[4\text{Fe-4S}]^{1+}$ cluster being a transient intermediate in the reductive cluster degradation pathway, as increasing the reaction time before freezing resulted in progressively decreasing spin quantification.

Incorporation of clusters on NFU4 and NFU5 via cluster transfer from ISCA1a/2

Cluster transfer experiments involving $[2\text{Fe-2S}]^{2+}$ -GRXS15 and both as-purified $[2\text{Fe-2S}]^{2+}$ and reconstituted $[4\text{Fe-4S}]^{2+}$ cluster-bound forms of ISCA1a/2 were carried out to assess the cluster donor for NFU4 and NFU5. No cluster transfer was observed using either $[2\text{Fe-2S}]^{2+}$ -ISCA1a/2 or $[2\text{Fe-2S}]^{2+}$ -GRXS15 as cluster donors for apo NFU4/5, as evidenced by the unchanged $[2\text{Fe-2S}]^{2+}$ -ISCA1a/2 or $[2\text{Fe-2S}]^{2+}$ -GRXS15 CD spectra for 30 min after addition of a two-fold excess of apo-NFU4/5, data not shown. In contrast, $[4\text{Fe-4S}]^{2+}$ cluster transfer from ISCA1a/2 was shown to be

effective for incorporating $[4\text{Fe-4S}]^{2+}$ clusters in both NFU4 and NFU5 (Figs. 5 & 6). Reconstituted ISCA1a/2 containing 25% $[2\text{Fe-2S}]^{2+}$ -ISCA1a/2 and 75% $[4\text{Fe-4S}]^{2+}$ -ISCA1a/2 was used as the donor. Since $[4\text{Fe-4S}]^{2+}$ -ISCA1a/2 exhibits negligible visible CD, the CD spectrum of the donor arises solely from $[2\text{Fe-2S}]^{2+}$ -ISCA1a/2, which will remain unchanged during $[4\text{Fe-4S}]^{2+}$ cluster transfer, as the above results showed that the $[2\text{Fe-2S}]^{2+}$ cluster on ISCA1a/2 cannot be transferred to NFU4 or NFU5. Anaerobic $[4\text{Fe-4S}]^{2+}$ cluster transfer from reconstituted ISCA1a/2 to DTT-pretreated apo-NFU4 and -NFU5 with a 1:1 donor:acceptor ratio was 80-90% complete after 20 min (Figs. 5 & 6). Percent cluster transfer was assessed by the difference in CD intensity at 326 and 362 nm (corrected for the contribution from $[2\text{Fe-2S}]^{2+}$ -ISCA1a/2). Best fits to second-order kinetics yielded a rate constant of $9.1 \pm 0.9 \times 10^3 \text{ M}^{-1}\text{min}^{-1}$ for NFU4 and $7.0 \pm 0.7 \times 10^3 \text{ M}^{-1}\text{min}^{-1}$ for NFU5, based on the initial concentrations of $[4\text{Fe-4S}]^{2+}$ clusters on ISCA1a/2 and the apo-NFU4/5 dimers. Control studies showed no reaction for the reverse cluster transfer, see Fig. S2, indicating a unidirectional reaction and absorption studies showed no degradation of the $[4\text{Fe-4S}]^{2+}$ cluster on ISCA1a/2 in the absence of NFU4 or NFU5, over the time course of the reaction, indicating intact cluster transfer.

In summary, we conclude that the rapid, quantitative, and unidirectional cluster transfer from $[4\text{Fe-4S}]^{2+}$ -ISCA1a/2 to NFU4 and NFU5 is likely to be a physiologically relevant pathway in plants. In addition, the results indicated that ISCA1a/2 and not NFU4 or NFU5 are responsible for $[2\text{Fe-2S}]^{2+}$ to $[4\text{Fe-4S}]^{2+}$ cluster conversions in late stages of mitochondrial Fe-S cluster biogenesis and that NFU4 and NFU5 are obligate $[4\text{Fe-4S}]^{2+}$ cluster trafficking proteins.

Activation of *At ACO2* using cluster-loaded forms of *At ISCA1a/2*, *NFU4* and *NFU5*

The ability of $[4\text{Fe-4S}]$ cluster-loaded forms of ISCA1a/2, NFU4 and NFU5 and $[2\text{Fe-2S}]$ cluster-loaded ISCA1a/2 to promote maturation of apo mitochondrial aconitase, ACO2, was assessed by monitoring aconitase activity as a function of time, after addition of a 3-fold excess of $[4\text{Fe-4S}]^{2+}$ clusters or a 6-fold excess of $[2\text{Fe-2S}]^{2+}$ clusters. Only the $[4\text{Fe-4S}]$ cluster donors were effective in rapid

restoration of ACO2 activity, with second order rate constants of $3.0 \pm 0.3 \times 10^4 \text{ M}^{-1}\text{min}^{-1}$ for $[4\text{Fe-4S}]$ cluster transfer from ISCA1a/2 and $1.2 \pm 0.3 \times 10^4 \text{ M}^{-1}\text{min}^{-1}$ for $[4\text{Fe-4S}]$ cluster transfer from NFU4 and NFU5 (Fig. 7). Due to the similarity of results obtained for $[4\text{Fe-4S}]$ -NFU4 and $[4\text{Fe-4S}]$ -NFU5, only NFU5 data are shown. Both reactions are at least 10 times faster than those observed under the same conditions with equivalent amounts of Fe^{2+} and S^{2-} ions, indicating that both are a consequence of intact cluster transfer rather than cluster degradation and reassembly on ACO2. The negligible rate of restoration of aconitase activity using $[2\text{Fe-2S}]$ -ISCA1a/2 indicates that consecutive $[2\text{Fe-2S}]^{2+}$ cluster transfers followed by *in situ* 2-electron reductive coupling is not a viable mechanism for maturation of the aconitase $[4\text{Fe-4S}]$ cluster.

Discussion

In mitochondria, the maturation of Fe-S proteins depends on the ISC machinery. Unlike the *de novo* assembly of a $[2\text{Fe-2S}]$ cluster on Isu/ISCU, the molecular mechanisms involved in cluster conversion, trafficking and insertion in client proteins are less well characterized. In this work, we provide new insights into the biochemical properties and roles of mitochondrial NFU4 and NFU5 in the plant ISC machinery.

NFU proteins have emerged as a major class of Fe-S cluster carrier proteins capable of binding and trafficking $[2\text{Fe-2S}]^{2+}$ or $[4\text{Fe-4S}]^{2+}$ clusters that are bound by conserved CXXC motifs at the subunit interface of a homodimer. This is well illustrated in *Helicobacter pylori* Nfu (50) and by our previous work on Arabidopsis chloroplastic NFU2, which purify as $[2\text{Fe-2S}]^{2+}$ cluster-containing recombinant proteins when expressed in *E. coli*, and can be obtained in either a $[2\text{Fe-2S}]^{2+}$ or $[4\text{Fe-4S}]^{2+}$ cluster-bound form via anaerobic reconstitution of the apo-proteins (38). $[2\text{Fe-2S}]$ -NFU2 has been shown to be a competent $[2\text{Fe-2S}]^{2+}$ cluster donor for GRXS16 and chloroplast ferredoxin (38,51), whereas $[4\text{Fe-4S}]$ -NFU2 was shown to be the likely physiological $[4\text{Fe-4S}]^{2+}$ cluster donor for adenosine 5'-phosphosulfate reductase (38). However, as discussed below, $[2\text{Fe-2S}]$ cluster trafficking by NFU proteins may be restricted to the SUF systems for Fe-S cluster assembly in bacteria

and plastids, which function under higher levels of O₂.

In contrast, the human and yeast mitochondrial NFU proteins are part of the ISC machinery and have been proposed to function exclusively as [4Fe-4S]²⁺ cluster carrier proteins based on both *in vivo* and *in vitro* evidence (33-35,52-54). This hypothesis has recently been challenged in a series of five publications by Cowan and coworkers, which claim that human mitochondrial NFU1 is a [2Fe-2S]²⁺ cluster carrier protein, based on UV-visible absorption/CD and EPR data (55-59). This interpretation is incorrect, based on our characterization of the homologous mitochondrial *At* NFU4 and NFU5 as [4Fe-4S]²⁺ cluster-carrier proteins. The UV-visible absorption and CD spectra of reconstituted NFU4 and NFU5 are essentially the same as those reported for reconstituted human NFU1 (55). However, the resonance Raman spectra of reconstituted NFU4 and NFU5 and the EPR spectra of reduced samples, unambiguously demonstrate that these absorption and CD attributes are indicative of a [4Fe-4S]²⁺ cluster, not a [2Fe-2S]²⁺ cluster. Moreover, Mössbauer and NMR studies have also demonstrated that reconstituted human NFU1 exclusively contains a [4Fe-4S]²⁺ cluster (53,54). This reinterpretation necessitates a major re-evaluation of the results and conclusions made by Cowan and coworkers about human NFU1. The discovery that both NFU4 and NFU5 are [4Fe-4S]²⁺ cluster-binding proteins, coupled with our inability to assemble a [2Fe-2S]²⁺ cluster on NFU4 and NFU5, either by reconstitution or cluster transfer from [2Fe-2S]-ISCA1a/2 or [2Fe-2S]-GRXS15, is in accord with the statement that all mitochondrial NFU proteins function in [4Fe-4S]²⁺ cluster trafficking. Nevertheless, we cannot rule out the possibility that [4Fe-4S]²⁺ cluster assembly on NFU4/5 in plants can also occur via [2Fe-2S]²⁺ cluster transfer from a GRXS15/BOLA4 complex, as recently proposed for the formation of human mitochondrial [4Fe-4S]-NFU1 via [2Fe-2S]²⁺ clusters provided by a GLRX5/BOLA3 complex (60).

The identification of NFU4/5 partners among the late-acting ISC components was unexplored in plants prior to this work. We obtained robust data demonstrating a specific and direct physical interaction with ISCA1 isoforms. The observation of intact [4Fe-4S] cluster transfer from ISCA1a/2 to NFU4/5

validates this interaction and suggests that in such heterodimers, ISCA1 isoforms are likely responsible for NFU4/5 recruitment. An interaction between mitochondrial NFU and ISCA1 proteins has been also observed but not characterized in detail in other organisms. In pull-down experiments, only mouse ISCA1, not ISCA2, retained NFU1 (30). In contrast, pull-down experiments using yeast Nfu1 allowed isolation of both Isa1 and Isa2 (35). It is possible that Isa2 has been detected because of a complex with Isa1 as we proposed to explain the positive BiFC result obtained with ISCA2. The NFU-ATC interaction seems largely conserved in evolution. In fact, *E. coli* NfuA interacts with all three ATC proteins (IscA, SufA and ErpA) and the Arabidopsis chloroplastic NFU1-SUFA1 couple also forms a complex (36,42). Considering the differences in NFU domain organization, such conservation suggests that only the NFU domain is crucial for the interaction with ATCs. This is what we observed by Y2H since the NFU domain of NFU4/5 was sufficient to form a complex with ISCA1 proteins. However, the opposite was observed for *E. coli* NfuA, since the N-terminal ATC domain, which lacks conserved cysteine residues, was shown to promote interaction of NfuA with its target proteins (36). Hence, the molecular function of the additional N-terminal domain found in mitochondrial NFUs remains to be further characterized. The possibilities include roles in recruiting some specific [4Fe-4S] cluster-acceptor proteins, stabilizing the interactions once formed, or promoting complex dissociation after Fe-S cluster transfer.

Cluster transfer studies also implicate that ISCA proteins act upstream of NFUs since only a unidirectional transfer from [4Fe-4S]-ISCA1a/2 to apo-NFU4 and -NFU5 was observed. The second order rate constants for intact [4Fe-4S]²⁺ cluster transfer from [4Fe-4S]-ISCA1a/2 to NFU4 and NFU5, $9.1 \pm 0.9 \times 10^3 \text{ M}^{-1}\text{min}^{-1}$ and $7.0 \pm 0.7 \times 10^3 \text{ M}^{-1}\text{min}^{-1}$, respectively, are potentially physiologically relevant. However, these cluster transfers were obtained in the absence of mitochondrial IBA57.1. Previous results with human ISCA1/2 (25) argue against IBA57 playing a role in [4Fe-4S]²⁺ cluster assembly on ISCA1/2 heterodimers. Nevertheless, Iba57 has been shown to form a complex with Isa1/2 in yeast mitochondria and depletion of any of these proteins in human and yeast cells resulted in decreased activities of key [4Fe-4S] cluster-

containing enzymes (28,29). Therefore, IBA57 may be required for preventing oxidative degradation of the assembled [4Fe-4S]²⁺ cluster and/or facilitating [4Fe-4S]²⁺ cluster transfer to client proteins. Alternatively, recent *in vitro* studies of human proteins have shown the formation of an ISCA2-IBA57 heterocomplex with a bridging [2Fe-2S] that is resistant to oxidative degradation and is capable of activating aconitase (27). Unfortunately, our inability thus far to express IBA57.1 as a soluble protein has precluded *in vitro* experiments to investigate its role in plant mitochondrial Fe-S cluster biogenesis.

In light of the non-essential role of NFU1 in yeast and human mitochondria, as evidenced by partially defective Fe-S enzymes aconitase, succinate dehydrogenase, and lipoic acid synthase, in cells lacking NFU1 (33-35,61), we asked whether Arabidopsis ISCA1a/2 heterodimers function solely as [4Fe-4S]²⁺ cluster assembler proteins that supply downstream [4Fe-4S]²⁺ cluster-carrier proteins such as NFU4/5 or whether they also function in terminal [4Fe-4S]²⁺ cluster delivery to a subset of client enzymes. The *in vitro* cluster transfer results presented in this work suggest that the latter is correct, based on the ability of [4Fe-4S]-ISCA1a/2 to effect rapid maturation of ACO2 *via* intact cluster transfer (second order rate constant of $3.0 \pm 0.3 \times 10^4 \text{ M}^{-1} \text{ min}^{-1}$), in the absence of IBA57.1. In addition, [4Fe-4S]-NFU4 and [4Fe-4S]-NFU5 are shown to be viable alternative [4Fe-4S]²⁺ cluster donors for ACO2, albeit with slightly lower rates of cluster transfer (second order rate constants of $1.2 \pm 0.3 \times 10^4 \text{ M}^{-1} \text{ min}^{-1}$). Hence our *in vitro* results are consistent with a non-essential role for NFU proteins in plant mitochondria. Moreover, our cluster transfer studies also support mitochondrial aconitase maturation *via* intact [4Fe-4S]²⁺ cluster transfer, rather than a mechanism involving sequential transfer of two [2Fe-2S]²⁺ clusters followed by *in situ* reductive coupling, as recently proposed for human mitochondrial and cytosolic aconitase (57).

We now have a better picture of the [4Fe-4S] cluster trafficking and interprotein interactions among late-acting ISC components in plants (Fig. 8). The results provide evidence for intact [4Fe-4S] transfer from ISCA1a/2 heterodimer to NFU4 and NFU5, and show that ISCA1a/2 and NFU4/5 are competent for

maturation of client [4Fe-4S] cluster-containing proteins. The question of the roles of BOLA and IBA57 remain as well as the question of the Fe-S cluster donor for INDH.

Experimental procedures

Binary yeast two-hybrid assays

Yeast two-hybrid assays were carried out in the Gal4-based yeast two hybrid reporter strain CY306 (62). The sequences encoding late-acting ISC components devoid of their mitochondrial targeting sequences were cloned into the pGADT7 or pGBKT7 vector (Clontech) between the NdeI or NcoI and BamHI restriction sites (primers used are listed in the Table S1). Gene products result in a protein fusion with the Gal4 activation domain (AD) or Gal4 DNA binding domain (BD), respectively. Transformants were selected on yeast nitrogen base (YNB) medium (0.7% yeast extract w/o amino acids, 2% glucose, 2% agar) without tryptophan and leucine (-Trp-Leu). Interactions were observed as cells growing on YNB medium in the absence of histidine (-His-Trp-Leu) at 30°C. The strength of the interactions was evaluated by challenging growth in the presence of 2 or 5 mM of the competitive inhibitor of *HIS3* gene product 3-amino-1,2,4-triazole (3-AT). Images were taken 5 days after dotting (7μL per dot at an optical density of 0.05 at 600 nm). Results are representative of at least three independent experiments, each on two colonies per transformation event. All constructs producing fusion proteins were also assayed in control experiments after co-transformation with either a pGADT7 or pGBKT7 empty vector.

Bimolecular fluorescence complementation

The full-length open reading frames coding for ISCA and NFU proteins were amplified from *A. thaliana* leaf cDNAs with the primers presented in Table S1 and cloned in both pUC-SPYCE and pUC-SPYNE vectors using XbaI and XhoI containing primers (63). The constructs, placed under the control of a CaMV 35S promoter, consist of fusions of the proteins of interest at the N-terminus of non-fluorescent C- and N-terminal halves of YFP, respectively. *Arabidopsis* protoplasts were prepared and co-transfected with pUC-SPYNE and pUC-SPYCE construct pairs for 5 min in a PEG-

based medium as described in (64) without vacuum infiltration. Pairs of constructs involving one empty vector were also transfected to control that none of the protein assayed could restore YFP fluorescence in the absence of interacting partners. Prior confocal analyses, fluorescent staining of the mitochondria within cells was performed by incubating freshly transfected protoplasts in a W5 solution (64) containing 100 nM MitoTracker® Orange CMXRos (Invitrogen). The YFP fluorescence in *Arabidopsis* protoplasts was recorded between 520 and 550 nm with a SP8 laser scanning confocal microscope (Leica Microsystems, Wetzlar, Germany), after excitation with an argon laser at 514 nm. MitoTracker® Orange CMXRos fluorescence was recorded between 580 and 620 nm after excitation at 560 nm. The Leica LASX software was used to obtain images with and without maximum Z-stack intensity projection. Images were processed using the Adobe Photoshop software package. Results are representative of three independent bombardment experiments including the analysis of 10 to 20 cells per transformation event.

Analytical and spectroscopic methods

Protein concentrations were determined by the DC protein assay (Bio-Rad) using bovine serum albumin (Roche) as standard. Iron concentrations were determined colorimetrically using bathophenanthroline under reducing conditions after digesting proteins in 0.8% KMnO₄/0.2 M HCl. A calibration curve was constructed from a series of dilutions of a 1000 ppm atomic absorption iron standard.

The preparation and handling of anaerobic samples for spectroscopic studies and cluster transfer experiments were carried out inside a Vacuum Atmosphere glove box under argon atmosphere at an oxygen level of 2 ppm or below. UV-visible absorption spectra were recorded in sealed quartz cuvettes at room temperature using a Shimadzu-3101PC spectrophotometer. CD spectra were recorded in sealed quartz cuvettes using a Jasco J-715 spectropolarimeter. Resonance Raman samples were prepared under strictly anaerobic conditions and comprised 18- μ L frozen droplets of protein solutions (~2 mM in Fe-S clusters) mounted on the cold finger of an Air Products

Displex Model CSA-202E closed cycle refrigerator (Air Products, Allentown, PA). Resonance Raman spectra were recorded at 17 K using an Instrument SA Ramanor U1000 scanning spectrometer coupled with a Coherent Sabre argon ion laser. Spectra were recorded by photon counting for 1 s every 0.5 cm⁻¹, using 7 cm⁻¹ resolution, and each spectrum is the sum of 80-120 scans.

Cloning, overexpression in E. coli and purification of recombinant proteins

The cloning of NFU4 (At3g20970) and NFU5 (At1g51390) in pET3d was described previously (65). For cloning in pCDF Duet, ISCA1a (At2g16710) was subcloned from pET28a using the NcoI-BamHI restriction sites of pCDF Duet in which ISCA2 (At5g03905) was cloned in the NdeI-XhoI restriction sites. The *Arabidopsis* ACO2 (At4g26970) sequence was amplified using the following primers: ACO2 for 5' CCCCCCGTCTCCCATGGCTTCTGAGCA TTCCTACA 3' and ACO2 rev 5' CCCCTCGAGTTACTTGGCGCTCAAAC 3' and cloned in the NcoI-XhoI restriction sites of pET15b. Note that a BsmBI type II restriction enzyme was used in the ACO2 for primer to generate a compatible NcoI extremity.

The *E. coli* BL21 (DE3) strain was used to co-express ISCA1a/2 from pCDF-Duet ISCA1a/2 plasmid and the untagged ACO2, which was purified following a procedure described previously for *Azotobacter vinelandii* aconitase (44). The same strain containing the pSBET helper plasmid was used for the expression of untagged NFU4 and NFU5 which were purified aerobically as described previously (65).

In vitro iscS-mediated Fe-S cluster reconstitution experiments

Apo-ISCA1a/2 was prepared by treating the as-purified [2Fe-2S] cluster-containing ISCA1a/2 with a 50-fold excess of EDTA and a 20-fold excess of potassium ferricyanide under anaerobic conditions and removing the excess reagents by ultrafiltration dialysis using a YM10 membrane. Reconstitutions of Fe-S clusters on as-purified ISCA1a/2, NFU4, NFU5 and ACO2 were carried out under strictly anaerobic conditions. Each recombinant protein was incubated in the

presence of a 12-fold excess of FAS, a 12-fold excess of L-cysteine and a catalytic amount of IscS in the presence of 2 mM DTT for approximately 5h in the case of ISCA1a/2 heterocomplex, 50 min in the case of NFU4 and NFU5 and 180 min in the case of ACO2. In all cases, the reconstitution mixture was loaded onto a 10 mL Hitrap Q-Sepharose column (GE Healthcare), and the protein was eluted with an increasing salt gradient of 0–1 M NaCl. A single colored fraction containing predominantly [4Fe-4S]²⁺ cluster-bound ISCA1a/2, NFU4, NFU5 or ACO2 was eluted under an increasing NaCl gradient.

Fe-S cluster transfer assays monitored by UV-visible CD spectroscopy

The time courses of Fe-S cluster transfer from the cluster-bound donor to apo-acceptor were monitored at room temperature, under anaerobic conditions in 1-cm cuvettes using CD spectroscopy. In all cases, the apo-acceptor protein was incubated with 2 mM DTT for 30 min and repurified to remove DTT (DTT pretreatment), prior to initiation of the reaction by the addition of apo-protein to the donor protein solution. The CD spectrum was monitored until no further change was observed. Peak-to-trough or fixed wavelength changes in CD intensity were used to assess the extent of cluster transfer as a function of time. The data were fitted to second order kinetics using the Kinetiscope chemical kinetics simulator software package (IBM), based on the initial concentration of Fe-S clusters on the donor protein and the concentration of the apo-acceptor protein. The directionality of cluster transfer was assessed by repeating the reaction with cluster-bound acceptor as the donor and the apo-donor as the acceptor. The lability of the donor Fe-S center in the reaction mixture was assessed by monitoring the UV-visible absorption or CD spectrum of the donor, in the absence of the acceptor, over the time course of the reaction. The specific conditions for each cluster transfer reported in this work are given in the results section and in the figure legends.

Activation of apo-aconitase ACO2 using Fe-S cluster-loaded forms of ISCA1a/2, NFU4 and NFU5

The apo-form of ACO2 was obtained by incubating as-purified ACO2 with EDTA and potassium ferricyanide as described

previously (44,66). Activation mixtures contained 2.4 μM apo-ACO2 and [4Fe-4S] cluster-containing ISCA1a/2, NFU4 or NFU5, each 7.4 μM in [4Fe-4S]²⁺ clusters, in 100 mM Tris-HCl, pH 7.8. [4Fe-4S]²⁺ cluster concentrations on ISCA1a/2, NFU4 and NFU5 were assessed based on a molar extinction coefficient at 400 nm of 15.0 mM⁻¹cm⁻¹. The same procedure was used in attempts to activate ACO2 (2.4 μM) using [2Fe-2S] cluster-containing ISCA1a/2 (14.5 μM in [2Fe-2S]²⁺ clusters). The [2Fe-2S]²⁺ cluster concentration on ISCA1a/2 was assessed using a molar extinction coefficient at 420 nm of 7.5 mM⁻¹cm⁻¹. Activation mixtures were incubated at room temperature under anaerobic conditions, and 10 μL samples were withdrawn at different times and assayed for aconitase activity. Activity was measured spectrophotometrically at 240 nm by following the formation of *cis*-aconitate from citrate or isocitrate, using a molar absorption coefficient $\epsilon_{240} = 3400 \text{ mM}^{-1}\text{cm}^{-1}$ for *cis*-aconitate (45,67). Anaerobically reconstituted samples of ACO2 containing one [4Fe-4S] cluster per protein monomer were used to establish maximal specific activity.

Acknowledgements

This work was supported by a grant from the National Institutes of Health (R37GM62524 to M.K.J) and by the Agence Nationale de la Recherche as part of the "Investissements d'Avenir" program (ANR-11-LABX-0002-01, Lab of Excellence ARBRE; and ANR-15-IDEX-04-LUE, "Lorraine Université d'Excellence") and by grant no. ANR-2013-BSV6-0002-01. The authors would like to thank Carine Alcon and the Montpellier Rio-Imaging and PHIV platforms for expertise and assistance in confocal microscopy and Tiphaine Dhalleine for help in cloning and protein expression.

Conflict of interest

The authors declare that they have no conflicts of interest with the content of this article.

Author contributions

JC, NR, MKJ designed the research; TA, FV, JPT performed research; TA, JPT, NR, MKJ

wrote the draft of the paper. All authors have read and approved the manuscript.

Data availability

All data are contained within the manuscript.

References

1. Lill, R., and Muhlenhoff, U. (2006) Iron-sulfur protein biogenesis in eukaryotes: Components and mechanisms. *Annu. Rev. Cell Dev. Biol.* **22**, 457-486
2. Balk, J., and Schaedler, T. A. (2014) Iron cofactor assembly in plants. *Annu. Rev. Plant Biol.* **65**, 125-153
3. Przybyla-Toscano, J., Roland, M., Gaymard, F., Couturier, J., and Rouhier, N. (2018) Roles and maturation of iron-sulfur proteins in plastids. *J. Biol. Inorg. Chem.* **23**, 545-566
4. Couturier, J., Touraine, B., Briat, J. F., Gaymard, F., and Rouhier, N. (2013) The iron-sulfur cluster assembly machineries in plants: Current knowledge and open questions. *Front. Plant Sci.* **4**, 259
5. Lill, R., and Freibert, S. A. (2020) Mechanisms of mitochondrial iron-sulfur protein biogenesis. *Annu. Rev. Biochem.* **89**, 471-499
6. Adam, A. C., Bornhovd, C., Prokisch, H., Neupert, W., and Hell, K. (2006) The Nfs1 interacting protein Isd11 has an essential role in Fe/S cluster biogenesis in mitochondria. *EMBO J.* **25**, 174-183
7. Van Vranken, J. G., Jeong, M. Y., Wei, P., Chen, Y. C., Gygi, S. P., Winge, D. R., and Rutter, J. (2016) The mitochondrial acyl carrier protein (ACP) coordinates mitochondrial fatty acid synthesis with iron sulfur cluster biogenesis. *eLife* **5**, e17828
8. Cory, S. A., Van Vranken, J. G., Brignole, E. J., Patra, S., Winge, D. R., Drennan, C. L., Rutter, J., and Barondeau, D. P. (2017) Structure of human Fe-S assembly subcomplex reveals unexpected cysteine desulfurase architecture and acyl-ACP-ISD11 interactions. *Proc. Natl. Acad. Sci. U. S. A.* **114**, E5325-E5334
9. Boniecki, M. T., Freibert, S. A., Muhlenhoff, U., Lill, R., and Cygler, M. (2017) Structure and functional dynamics of the mitochondrial Fe/S cluster synthesis complex. *Nat. Commun.* **8**, 1287
10. Colin, F., Martelli, A., Clemancey, M., Latour, J. M., Gambarelli, S., Zeppieri, L., Birck, C., Page, A., Puccio, H., and Ollagnier de Choudens, S. (2013) Mammalian frataxin controls sulfur production and iron entry during de novo Fe₄S₄ cluster assembly. *J. Am. Chem. Soc.* **135**, 733-740
11. Parent, A., Elduque, X., Cornu, D., Belot, L., Le Caer, J. P., Grandas, A., Toledano, M. B., and D'Autreaux, B. (2015) Mammalian frataxin directly enhances sulfur transfer of NFS1 persulfide to both ISCU and free thiols. *Nat. Commun.* **6**, 5686
12. Fox, N. G., Yu, X., Feng, X., Bailey, H. J., Martelli, A., Nabhan, J. F., Strain-Damerell, C., Bulawa, C., Yue, W. W., and Han, S. (2019) Structure of the human frataxin-bound iron-sulfur cluster assembly complex provides insight into its activation mechanism. *Nat. Commun.* **10**, 2210
13. Gervason, S., Larkem, D., Mansour, A. B., Botzanowski, T., Muller, C. S., Pecqueur, L., Le Pavec, G., Delaunay-Moisan, A., Brun, O., Agramunt, J., Grandas, A., Fontecave, M., Schunemann, V., Cianferani, S., Sizun, C., Toledano, M. B., and D'Autreaux, B. (2019) Physiologically relevant reconstitution of iron-sulfur cluster biosynthesis uncovers persulfide-processing functions of ferredoxin-2 and frataxin. *Nat. Commun.* **10**, 3566
14. Weibert, H., Freibert, S. A., Gallo, A., Heidenreich, T., Linne, U., Amlacher, S., Hurt, E., Muhlenhoff, U., Banci, L., and Lill, R. (2014) Functional reconstitution of mitochondrial Fe/S cluster synthesis on Isu1 reveals the involvement of ferredoxin. *Nat. Commun.* **5**, 5013
15. Maio, N., Jain, A., and Rouault, T. A. (2020) Mammalian iron-sulfur cluster biogenesis: Recent insights into the roles of frataxin, acyl carrier protein and ATPase-mediated transfer to recipient proteins. *Curr. Opin. Chem. Biol.* **55**, 34-44

16. Mühlhoff, U., Gerber, J., Richhardt, N., and Lill, R. (2003) Components involved in assembly and dislocation of iron-sulfur clusters on the scaffold protein Isu1p. *EMBO J.* **22**, 4815-4825
17. Vickery, L. E., and Cupp-Vickery, J. R. (2007) Molecular chaperones HscA/Ssq1 and HscB/Jac1 and their roles in iron-sulfur protein maturation. *Crit. Rev. Biochem. Mol. Biol.* **42**, 95-111
18. Uzarska, M. A., Dutkiewicz, R., Freibert, S. A., Lill, R., and Mühlhoff, U. (2013) The mitochondrial Hsp70 chaperone Ssq1 facilitates Fe/S cluster transfer from Isu1 to Grx5 by complex formation. *Mol. Biol. Cell* **24**, 1830-1841
19. Moseler, A., Aller, I., Wagner, S., Nietzel, T., Przybyla-Toscano, J., Mühlhoff, U., Lill, R., Berndt, C., Rouhier, N., Schwarzlander, M., and Meyer, A. J. (2015) The mitochondrial monothiol glutaredoxin S15 is essential for iron-sulfur protein maturation in *Arabidopsis thaliana*. *Proc. Natl. Acad. Sci. U. S. A.* **112**, 13735-13740
20. Wydro, M. M., Sharma, P., Foster, J. M., Bych, K., Meyer, E. H., and Balk, J. (2013) The evolutionarily conserved iron-sulfur protein INDH is required for complex I assembly and mitochondrial translation in *Arabidopsis* [corrected]. *Plant Cell* **25**, 4014-4027
21. Bych, K., Kerscher, S., Netz, D. J., Pierik, A. J., Zwicker, K., Huynen, M. A., Lill, R., Brandt, U., and Balk, J. (2008) The iron-sulphur protein Ind1 is required for effective complex I assembly. *EMBO J.* **27**, 1736-1746
22. Couturier, J., Wu, H. C., Dhalleine, T., Pegeot, H., Sudre, D., Gualberto, J. M., Jacquot, J. P., Gaymard, F., Vignols, F., and Rouhier, N. (2014) Monothiol glutaredoxin-BolA interactions: Redox control of *Arabidopsis thaliana* BolA2 and SufE1. *Mol. Plant* **7**, 187-205
23. Gelling, C., Dawes, I. W., Richhardt, N., Lill, R., and Mühlhoff, U. (2008) Mitochondrial Iba57p is required for Fe/S cluster formation on aconitase and activation of radical SAM enzymes. *Mol. Cell Biol.* **28**, 1851-1861
24. Banci, L., Brancaccio, D., Ciofi-Baffoni, S., Del Conte, R., Gadepalli, R., Mikolajczyk, M., Neri, S., Piccioli, M., and Winkelman, J. (2014) [2Fe-2S] cluster transfer in iron-sulfur protein biogenesis. *Proc. Natl. Acad. Sci. U. S. A.* **111**, 6203-6208
25. Brancaccio, D., Gallo, A., Mikolajczyk, M., Zovo, K., Palumaa, P., Novellino, E., Piccioli, M., Ciofi-Baffoni, S., and Banci, L. (2014) Formation of [4Fe-4S] clusters in the mitochondrial iron-sulfur cluster assembly machinery. *J. Am. Chem. Soc.* **136**, 16240-16250
26. Nasta, V., Giachetti, A., Ciofi-Baffoni, S., and Banci, L. (2017) Structural insights into the molecular function of human [2Fe-2S] BOLA1-GRX5 and [2Fe-2S] BOLA3-GRX5 complexes. *Biochim. Biophys. Acta* **1861**, 2119-2131
27. Gourdupis, S., Nasta, V., Calderone, V., Ciofi-Baffoni, S., and Banci, L. (2018) IBA57 recruits ISCA2 to form a [2Fe-2S] cluster-mediated complex. *J. Am. Chem. Soc.* **140**, 14401-14412
28. Mühlhoff, U., Richter, N., Pines, O., Pierik, A. J., and Lill, R. (2011) Specialized function of yeast Isa1 and Isa2 proteins in the maturation of mitochondrial [4Fe-4S] proteins. *J. Biol. Chem.* **286**, 41205-41216
29. Sheftel, A. D., Wilbrecht, C., Stehling, O., Niggemeyer, B., Elsasser, H. P., Mühlhoff, U., and Lill, R. (2012) The human mitochondrial ISCA1, ISCA2, and IBA57 proteins are required for [4Fe-4S] protein maturation. *Mol. Biol. Cell* **23**, 1157-1166
30. Beilschmidt, L. K., Ollagnier de Choudens, S., Fournier, M., Sanakis, I., Hograindleur, M. A., Clemancey, M., Blondin, G., Schmucker, S., Eisenmann, A., Weiss, A., Koebel, P., Messaddeq, N., Puccio, H., and Martelli, A. (2017) ISCA1 is essential for mitochondrial Fe₄S₄ biogenesis *in vivo*. *Nat. Commun.* **8**, 15124
31. Sheftel, A. D., Stehling, O., Pierik, A. J., Netz, D. J., Kerscher, S., Elsasser, H. P., Wittig, I., Balk, J., Brandt, U., and Lill, R. (2009) Human ind1, an iron-sulfur cluster assembly factor for respiratory complex I. *Mol. Cell Biol.* **29**, 6059-6073
32. Calvo, S. E., Tucker, E. J., Compton, A. G., Kirby, D. M., Crawford, G., Burt, N. P., Rivas, M., Guiducci, C., Bruno, D. L., Goldberger, O. A., Redman, M. C., Wiltshire, E., Wilson, C. J., Altshuler, D., Gabriel, S. B., Daly, M. J., Thorburn, D. R., and Mootha, V. K. (2010) High-throughput, pooled sequencing identifies mutations in NUBPL and FOXRED1 in human complex I deficiency. *Nat. Genet.* **42**, 851-858

33. Navarro-Sastre, A., Tort, F., Stehling, O., Uzarska, M. A., Arranz, J. A., Del Toro, M., Labayru, M. T., Landa, J., Font, A., Garcia-Villoria, J., Merinero, B., Ugarte, M., Gutierrez-Solana, L. G., Campistol, J., Garcia-Cazorla, A., Vaquerizo, J., Riudor, E., Briones, P., Elpeleg, O., Ribes, A., and Lill, R. (2011) A fatal mitochondrial disease is associated with defective NFU1 function in the maturation of a subset of mitochondrial Fe-S proteins. *Am. J. Hum. Genet.* **89**, 656-667
34. Cameron, J. M., Janer, A., Levandovskiy, V., Mackay, N., Rouault, T. A., Tong, W. H., Ogilvie, I., Shoubridge, E. A., and Robinson, B. H. (2011) Mutations in iron-sulfur cluster scaffold genes NFU1 and BOLA3 cause a fatal deficiency of multiple respiratory chain and 2-oxoacid dehydrogenase enzymes. *Am. J. Hum. Genet.* **89**, 486-495
35. Melber, A., Na, U., Vashisht, A., Weiler, B. D., Lill, R., Wohlschlegel, J. A., and Winge, D. R. (2016) Role of Nfu1 and Bol3 in iron-sulfur cluster transfer to mitochondrial clients. *eLife* **5**, e15991
36. Py, B., Gerez, C., Angelini, S., Planel, R., Vinella, D., Loiseau, L., Talla, E., Brochier-Armanet, C., Garcia Serres, R., Latour, J. M., Ollagnier-de Choudens, S., Fontecave, M., and Barras, F. (2012) Molecular organization, biochemical function, cellular role and evolution of NfuA, an atypical Fe-S carrier. *Mol. Microbiol.* **86**, 155-171
37. Leon, S., Touraine, B., Ribot, C., Briat, J. F., and Lobreaux, S. (2003) Iron-sulphur cluster assembly in plants: Distinct NFU proteins in mitochondria and plastids from *Arabidopsis thaliana*. *Biochem. J.* **371**, 823-830
38. Gao, H., Subramanian, S., Couturier, J., Naik, S. G., Kim, S. K., Leustek, T., Knaff, D. B., Wu, H. C., Vignols, F., Huynh, B. H., Rouhier, N., and Johnson, M. K. (2013) *Arabidopsis thaliana* Nfu2 accommodates [2Fe-2S] or [4Fe-4S] clusters and is competent for *in vitro* maturation of chloroplast [2Fe-2S] and [4Fe-4S] cluster-containing proteins. *Biochemistry* **52**, 6633-6645
39. Gao, H., Azam, T., Randeniya, S., Couturier, J., Rouhier, N., and Johnson, M. K. (2018) Function and maturation of the Fe-S center in dihydroxyacid dehydratase from *Arabidopsis*. *J. Biol. Chem.* **293**, 4422-4433
40. Touraine, B., Vignols, F., Przybyla-Toscano, J., Ischebeck, T., Dhalleine, T., Wu, H. C., Magno, C., Berger, N., Couturier, J., Dubos, C., Feussner, I., Caffarri, S., Havaux, M., Rouhier, N., and Gaymard, F. (2019) Iron-sulfur protein NFU2 is required for branched-chain amino acid synthesis in *Arabidopsis* roots. *J. Exp. Bot.* **70**, 1875-1889
41. Berger, N., Vignols, F., Przybyla-Toscano, J., Roland, M., Rofidal, V., Touraine, B., Zienkiewicz, K., Couturier, J., Feussner, I., Santoni, V., Rouhier, N., Gaymard, F., and Dubos, C. (2020) Identification of client iron-sulfur proteins of the chloroplastic NFU2 transfer protein in *Arabidopsis thaliana*. *J. Exp. Bot.* **71**, 4171-4187
42. Roland, M., Przybyla-Toscano, J., Vignols, F., Berger, N., Azam, T., Christ, L., Santoni, V., Wu, H. C., Dhalleine, T., Johnson, M. K., Dubos, C., Couturier, J., and Rouhier, N. (2020) The plastidial *Arabidopsis thaliana* NFU1 protein binds and delivers [4Fe-4S] clusters to specific client proteins. *J. Biol. Chem.* **295**, 1727-1742
43. Uzarska, M. A., Przybyla-Toscano, J., Spantgar, F., Zannini, F., Lill, R., Mühlenhoff, U., and Rouhier, N. (2018) Conserved functions of *Arabidopsis* mitochondrial late-acting maturation factors in the trafficking of iron-sulfur clusters. *Biochim. Biophys. Acta* **1865**, 1250-1259
44. Chandramouli, K., Unciuleac, M. C., Naik, S., Dean, D. R., Huynh, B. H., and Johnson, M. K. (2007) Formation and properties of [4Fe-4S] clusters on the IscU scaffold protein. *Biochemistry* **46**, 6804-6811
45. Bandyopadhyay, S., Naik, S. G., O'Carroll, I. P., Huynh, B. H., Dean, D. R., Johnson, M. K., and Dos Santos, P. C. (2008) A proposed role for the *Azotobacter vinelandii* NfuA protein as an intermediate iron-sulfur cluster carrier. *J. Biol. Chem.* **283**, 14092-14099
46. Agar, J. N., Krebs, C., Frazzon, J., Huynh, B. H., Dean, D. R., and Johnson, M. K. (2000) IscU as a scaffold for iron-sulfur cluster biosynthesis: sequential assembly of [2Fe-2S] and [4Fe-4S] clusters in IscU. *Biochemistry* **39**, 7856-7862
47. Zhang, B., Crack, J. C., Subramanian, S., Green, J., Thomson, A. J., Le Brun, N. E., and Johnson, M. K. (2012) Reversible cycling between cysteine persulfide-ligated [2Fe-2S] and cysteine-

- ligated [4Fe-4S] clusters in the FNR regulatory protein. *Proc. Natl. Acad. Sci. U. S. A.* **109**, 15734-15739
48. Czernuszewicz, R. S., Macor, K. A., Johnson, M. K., Gewirth, A., and Spiro, T. G. (1987) Vibrational mode structure and symmetry in proteins and analogs containing Fe₄S₄ clusters: Resonance Raman evidence that HiPIP is tetrahedral while ferredoxin undergoes a D_{2d} distortion. *J. Am. Chem. Soc.* **109**, 7178-7187
 49. Brereton, P. S., Duderstadt, R. E., Staples, C. R., Johnson, M. K., and Adams, M. W. (1999) Effect of serinate ligation at each of the iron sites of the [Fe₄S₄] cluster of *Pyrococcus furiosus* ferredoxin on the redox, spectroscopic, and biological properties. *Biochemistry* **38**, 10594-10605
 50. Benoit, S. L., Holland, A. A., Johnson, M. K., and Maier, R. J. (2018) Iron-sulfur protein maturation in *Helicobacter pylori*: Identifying a Nfu-type cluster carrier protein and its iron-sulfur protein targets. *Mol. Microbiol.* **108**, 379-396
 51. Yabe, T., Morimoto, K., Kikuchi, S., Nishio, K., Terashima, I., and Nakai, M. (2004) The *Arabidopsis* chloroplastic NifU-like protein CnfU, which can act as an iron-sulfur cluster scaffold protein, is required for biogenesis of ferredoxin and photosystem I. *Plant Cell* **16**, 993-1007
 52. Braymer, J. J., and Lill, R. (2017) Iron-sulfur cluster biogenesis and trafficking in mitochondria. *J. Biol. Chem.* **292**, 12754-12763
 53. Tong, W. H., Jameson, G. N., Huynh, B. H., and Rouault, T. A. (2003) Subcellular compartmentalization of human Nfu, an iron-sulfur cluster scaffold protein, and its ability to assemble a [4Fe-4S] cluster. *Proc. Natl. Acad. Sci. U. S. A.* **100**, 9762-9767
 54. Cai, K., Liu, G., Frederick, R. O., Xiao, R., Montelione, G. T., and Markley, J. L. (2016) Structural/functional properties of human NFU1, an intermediate [4Fe-4S] carrier in human mitochondrial iron-sulfur cluster biogenesis. *Structure* **24**, 2080-2091
 55. Wachnowsky, C., Fidai, I., and Cowan, J. A. (2016) Iron-sulfur cluster exchange reactions mediated by the human Nfu protein. *J. Biol. Inorg. Chem.* **21**, 825-836
 56. Wachnowsky, C., Liu, Y., Yoon, T., and Cowan, J. A. (2018) Regulation of human Nfu activity in Fe-S cluster delivery-characterization of the interaction between Nfu and the HSPA9/Hsc20 chaperone complex. *FEBS J.* **285**, 391-410
 57. Wachnowsky, C., Hendricks, A. L., Wesley, N. A., Ferguson, C., Fidai, I., and Cowan, J. A. (2019) Understanding the mechanism of [4Fe-4S] cluster assembly on eukaryotic mitochondrial and cytosolic aconitase. *Inorg. Chem.* **58**, 13686-13695
 58. Wesley, N. A., Wachnowsky, C., Fidai, I., and Cowan, J. A. (2017) Analysis of NFU-1 metallocofactor binding-site substitutions-impacts on iron-sulfur cluster coordination and protein structure and function. *FEBS J.* **284**, 3817-3837
 59. Wesley, N. A., Wachnowsky, C., Fidai, I., and Cowan, J. A. (2017) Understanding the molecular basis for multiple mitochondrial dysfunctions syndrome 1 (MMDS1): Impact of a disease-causing Gly189Arg substitution on NFU1. *FEBS J.* **284**, 3838-3848
 60. Nasta, V., Suraci, D., Gourdoups, S., Ciofi-Baffoni, S., and Banci, L. (2020) A pathway for assembling [4Fe-4S]⁽²⁺⁾ clusters in mitochondrial iron-sulfur protein biogenesis. *FEBS J.* **287**, 2312-2327
 61. Uzarska, M. A., Nasta, V., Weiler, B. D., Spantgar, F., Ciofi-Baffoni, S., Saviello, M. R., Gonnelli, L., Muhlenhoff, U., Banci, L., and Lill, R. (2016) Mitochondrial Bol1 and Bol3 function as assembly factors for specific iron-sulfur proteins. *eLife* **5**, e16673
 62. Vignols, F., Bréhélin, C., Surdin-Kerjan, Y., Thomas, D., and Meyer, Y. (2005) A yeast two-hybrid knockout strain to explore thioredoxin-interacting proteins *in vivo*. *Proc. Nat. Acad. Sci. U. S. A.* **102**, 16729-16734
 63. Walter, M., Chaban, C., Schütze, K., Batistic, O., Weckermann, K., Näke, C., Blazevic, D., Grefen, C., Schumacher, K., Oecking, C., Harter, K., and Kudla, J. (2004) Visualization of protein interactions in living plant cells using bimolecular fluorescence complementation. *Plant J.* **40**, 428-438

64. Yoo, S. D., Cho, Y. H., and Sheen, J. (2007) *Arabidopsis* mesophyll protoplasts: a versatile cell system for transient gene expression analysis. *Nat. Protoc.* **2**, 1565-1572
65. Zannini, F., Roret, T., Przybyla-Toscano, J., Dhalleine, T., Rouhier, N., and Couturier, J. (2018) Mitochondrial *Arabidopsis thaliana* TRXo isoforms bind an iron-sulfur cluster and reduce NFU proteins *in vitro*. *Antioxidants (Basel)* **7**, 142
66. Kennedy, M. C., and Beinert, H. (1988) The state of cluster SH and S²⁻ of aconitase during cluster interconversions and removal. A convenient preparation of apoenzyme. *J. Biol. Chem.* **263**, 8194-8198
67. Unciuleac, M. C., Chandramouli, K., Naik, S., Mayer, S., Huynh, B. H., Johnson, M. K., and Dean, D. R. (2007) *In vitro* activation of apo-aconitase using a [4Fe-4S] cluster-loaded form of the IscU [Fe-S] cluster scaffolding protein. *Biochemistry* **46**, 6812-6821
68. Fu, W. G., Morgan, T. V., Mortenson, L. E., and Johnson, M. K. (1991) Resonance Raman studies of the [4Fe-4S] to [2Fe-2S] cluster conversion in the iron protein of nitrogenase. *FEBS Lett.* **284**, 165-168

Table 1. Fe-S stretching frequencies (cm^{-1}) and vibrational assignments for the $[\text{4Fe-4S}]^{2+}$ centers in *C. pasterianum* 8Fe Fd, *C. pasterianum* N₂ase Fe-protein, *A. thaliana* NFU4, and *A. thaliana* NFU5.

Assignments under T _d symmetry ^a	<i>C. pasterianum</i> 8Fe Ferredoxin ^b	<i>C. pasterianum</i> N ₂ ase Fe-protein ^c	<i>A. thaliana</i> NFU4	<i>A. thaliana</i> NFU5
Mainly Terminal $\nu(\text{Fe-S}^{\text{t}})$				
A ₁	395	391	409 or 388	405 or 387
T ₂	363, 351	356	358	358
Mainly Bridging $\nu(\text{Fe-S}^{\text{b}})$				
T ₂	380	391	388	387
A ₁	338	335	338	338
E	298, 276	281	299, 288	299, 288
T ₁	276, 266	265	288, 277	288, 274
T ₂	251	248	252	252

^aSymmetry labels assuming idealized T_d symmetry for the Fe₄S₄^bS₄^t core, where Fe-S^b and Fe-S^t indicate bridging and terminal stretching, respectively.

^bTaken from Ref. (48)

^cTaken from Ref. (68)

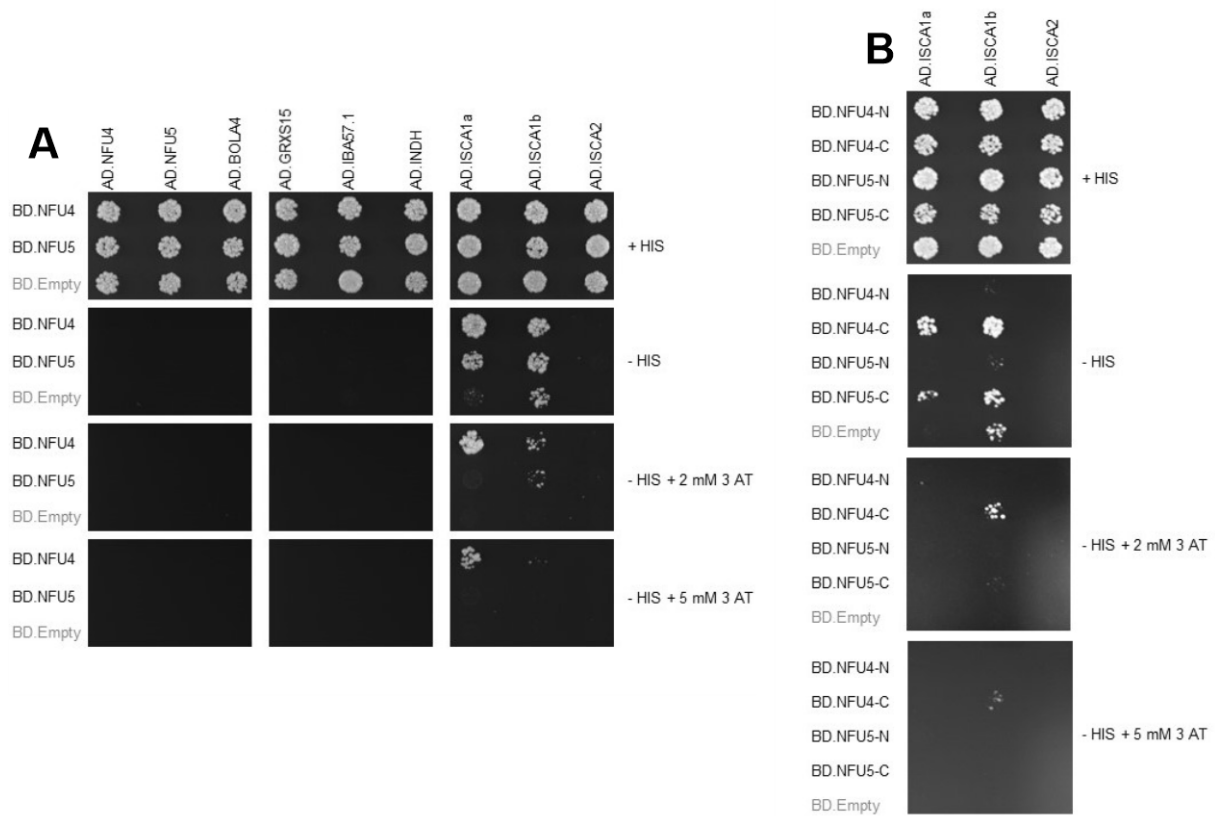


Figure 1. Binary Y2H interaction between Arabidopsis NFU4 and NFU5 and other late-acting ISC components. A. The yeast strain CY306 was co-transformed with sequences encoding the mature forms of NFU4 and NFU5 proteins fused at the C-terminus of the Gal4 DNA-binding domain (BD) as indicated and other ISC components fused at the C-terminus of the Gal4 activation domain (AD). The co-transformed yeast cells were plated on a control medium containing histidine (+ HIS) and interactions were tested on medium without histidine (- HIS) in the presence of 2 mM or 5 mM 3-amino-1,2,4-triazole (3-AT) as indicated. Yeast growth was analyzed after 5 days. Only AtISCA1b exhibited a slight auto-activation in the -His medium which disappeared in the presence of 3-AT. No autoactivation was observed for BD-NFU4 and NFU5 (not shown). B. The yeast strain CY306 was co-transformed with sequences encoding the N- or C-terminal domains of NFU4 and NFU5 proteins fused at the C-terminus of the Gal4 DNA-binding domain (BD) and ISCA1a or ISCA1b fused at the C-terminus of the Gal4 activation domain (AD). The NFU4-N and -C domains correspond respectively to amino acids 80 to 168 and 187 to 283 of NFU4 whereas the NFU5-N and -C domains correspond respectively to amino acid 75 to 163 and 182 to 275 of NFU5. The conditions are as in (A).

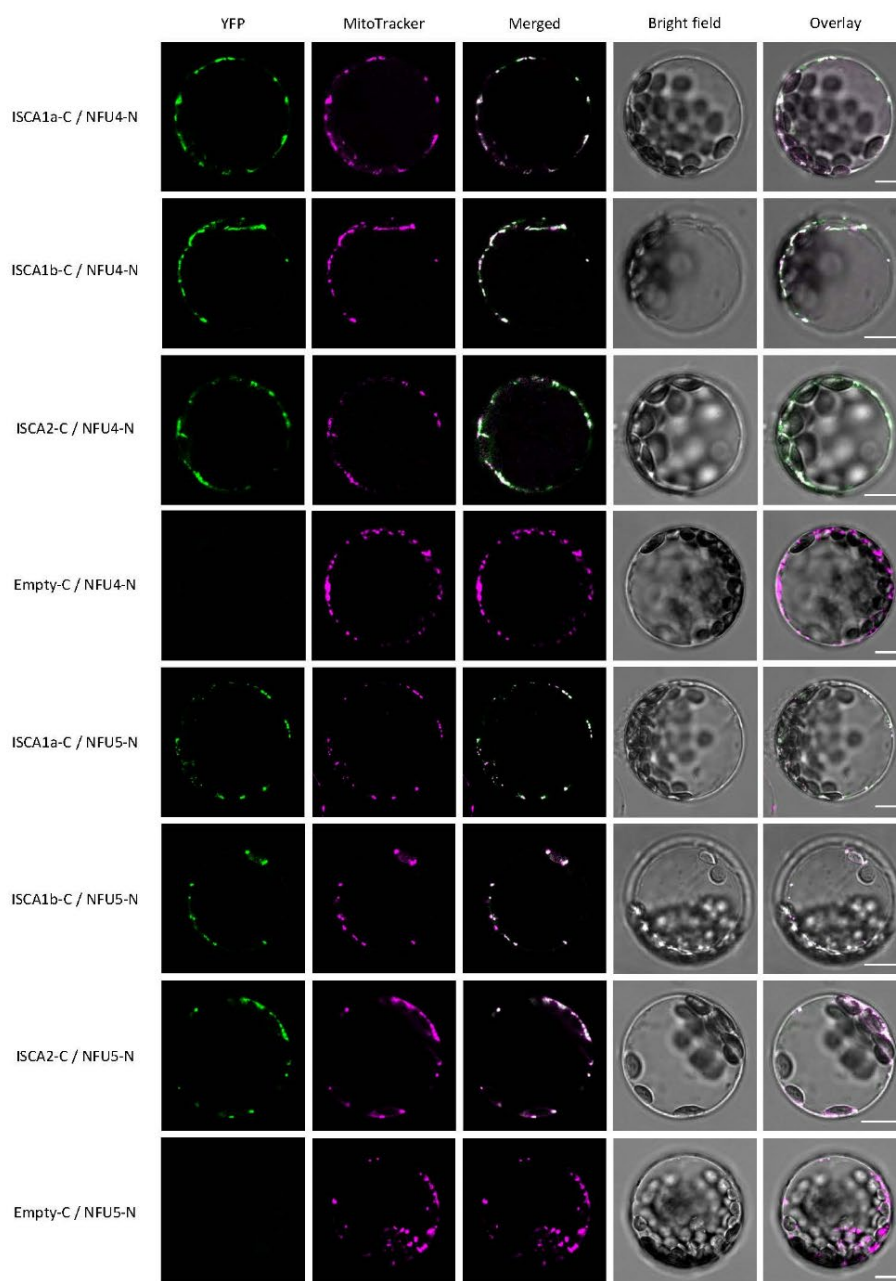


Figure 2. BiFC interactions between Arabidopsis mitochondrial ISCA and NFUs. Arabidopsis protoplasts isolated from 4 week-old plantlets were transfected with combinations of two vectors expressing either NFU4 or NFU5 fused to the N-terminal region of the YFP protein (NFUs-N in panels) and ISCA-C fused to the C-terminal region of YFP (ISCA-C in panels). The YFP fluorescence was recorded 24h post-transfection by confocal microscopy. Negative controls verifying that none of the NFU proteins tested alone with the empty partner vector can restore YFP fluorescence are shown as Empty-C/NFUs-N in panels, those verifying ISCA-C/Empty-N combinations are shown in Fig. S1. Protoplast co-transfections using opposite protein chimera (ISCA-N with NFUs-C) provided similar patterns but also showed a strong tendency to form cytosolic aggregates (not shown). All images were captured using the LAS X software at confocal plans at selected Z dimensions and processed using the Adobe Photoshop software. Results are representative of three independent bombardment experiments including the analysis of 10 to 20 cells per transformation event. YFP, yellow fluorescent protein. MitoTracker® Orange CMXRos (Invitrogen) was used at 100 nM to label mitochondria within cells. Bars = 10 μ m.

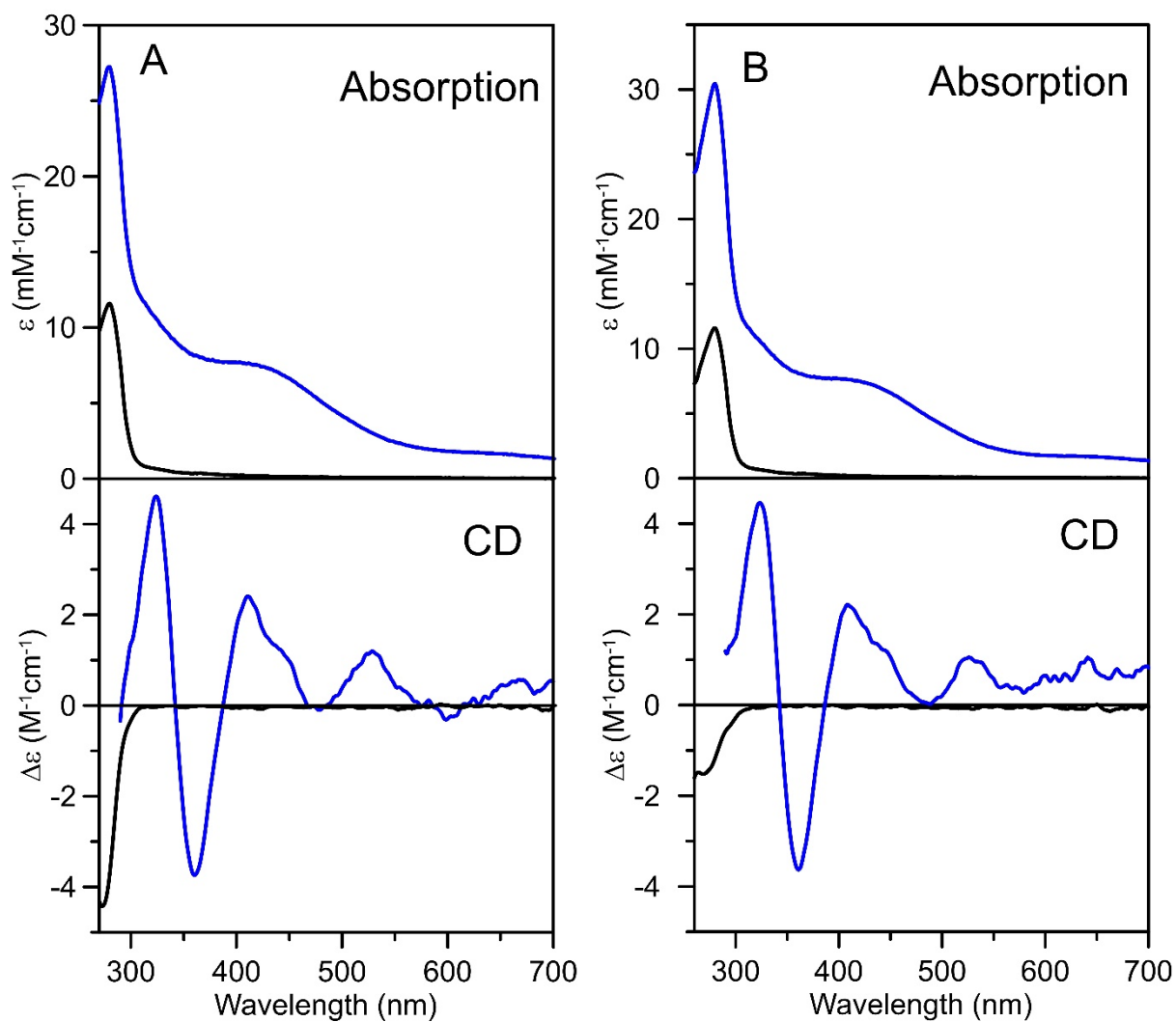


Figure 3. Room temperature UV-visible absorption spectra and CD spectra of *At* NFU4 and *At* NFU5. As-purified apo-NFU4 and NFU5 are shown as black lines and reconstituted NFU4 (A) and NFU5 (B) are shown as blue lines. All ϵ and $\Delta\epsilon$ values are based on NFU4 and NFU5 protein monomer concentration.

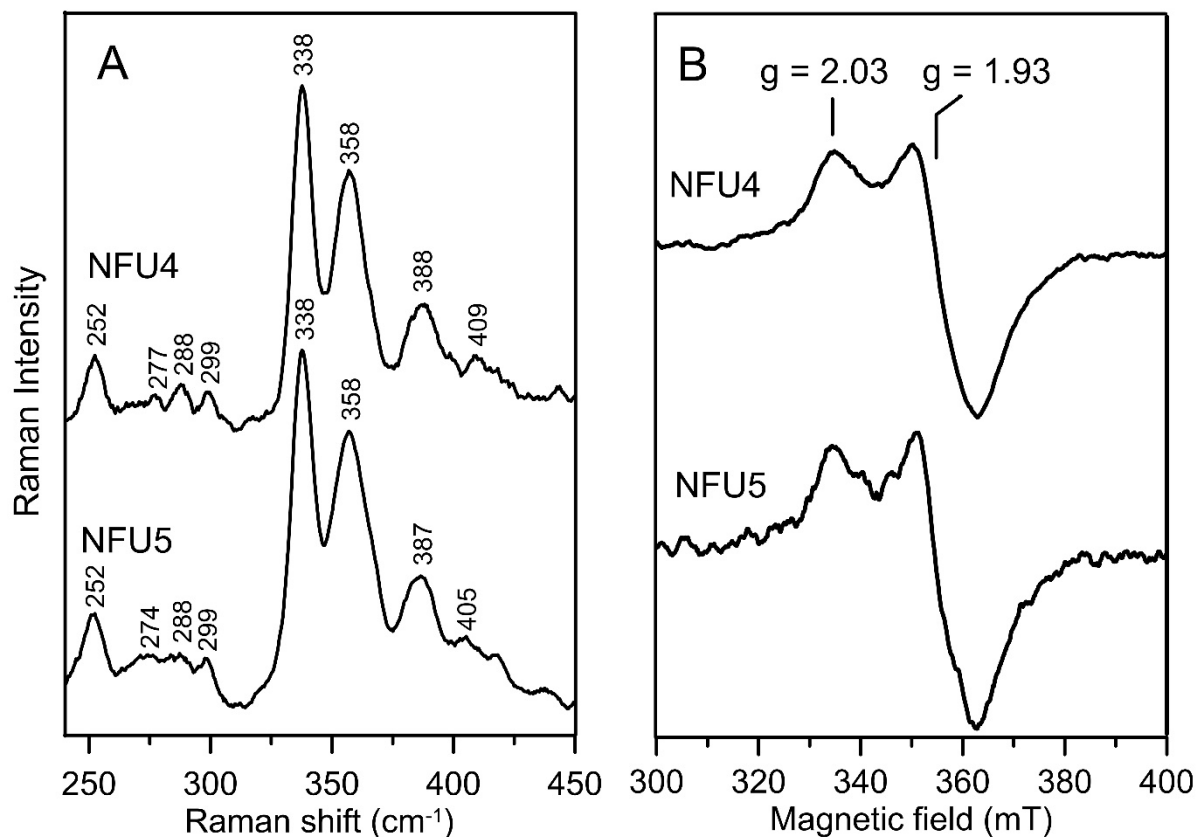


Figure 4. Comparison of the resonance Raman and EPR spectra of reconstituted *At* NFU4 and *At* NFU5. A. Resonance Raman spectra of reconstituted NFU4 and NFU5 recorded at 17 K with 457.9-nm excitation. Each spectrum is the sum of 100 individual scans, with each scan involving photon counting for 1 s at 0.5 cm⁻¹ increments, with 7 cm⁻¹ spectral resolution. Bands due to frozen buffer solution have been subtracted from both spectra. B. X-band EPR spectra of reconstituted NFU4 and NFU5 reduced with one reducing equivalent of dithionite and frozen immediately in liquid nitrogen. EPR conditions: microwave frequency, 9.60 GHz; microwave power, 10 mW; modulation amplitude, 0.63 mT; temperature, 10 K.

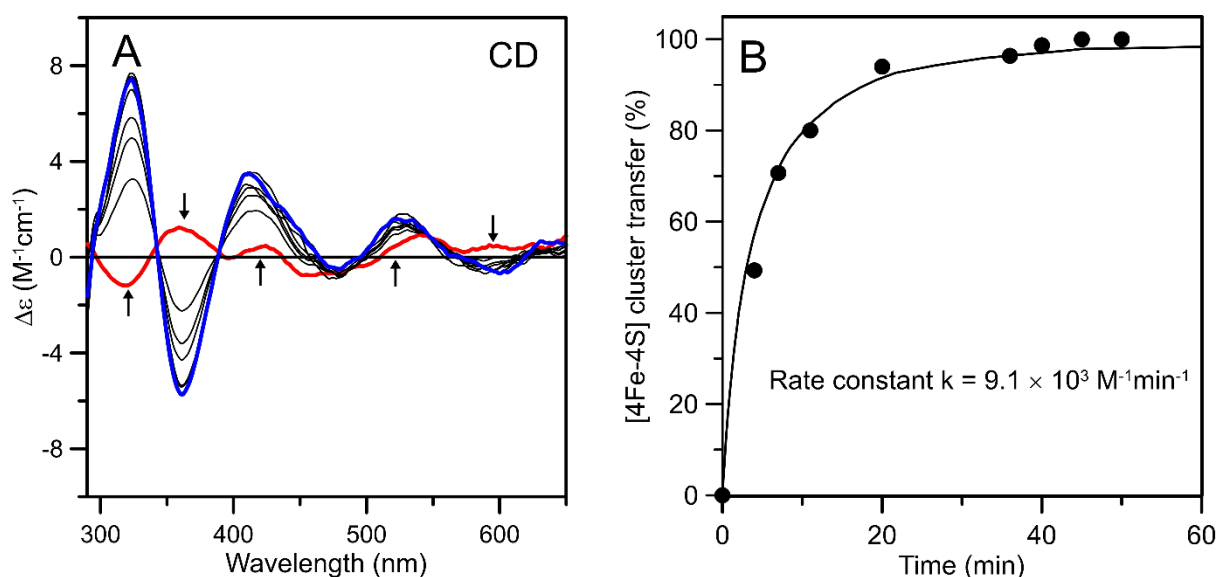


Figure 5. Cluster transfer from *At* [4Fe-4S]²⁺-ISCA1a/2 to *At* apo-NFU4 monitored by CD spectroscopy as a function of time. (A) CD spectra of the cluster transfer reaction mixture that was initially 30 μM in ISCA1a/2 [4Fe-4S]²⁺ clusters and 60 μM in DTT-pretreated apo-NFU4 monomer. The thick red line corresponds to [4Fe-4S]²⁺-ISCA1a/2 recorded before addition of apo-NFU4 to the reaction mixture. The thin grey lines correspond to CD spectra recorded at 4, 7, 11, 20, 36, 40, 45, and 50 min after the addition of apo-NFU4. The thick blue line corresponds to complete [4Fe-4S]²⁺ cluster transfer to NFU4. The arrows indicate the direction of intensity change with increasing time and Δε values were calculated based on the initial concentration of [4Fe-4S]²⁺ clusters in the reaction mixture. The cluster transfer reaction was carried out under anaerobic conditions at room temperature in 100 mM Tris-HCl buffer at pH 7.8. (B) Kinetic simulation of cluster transfer from [4Fe-4S]²⁺-ISCA1a/2 to apo-NFU4 based on second-order kinetics and the initial concentrations of [4Fe-4S]²⁺ clusters on [4Fe-4S]²⁺-ISCA1a/2 and of apo-NFU4. Percent cluster transfer was assessed by the difference in CD intensity at 326 and 362 nm (black circles) and simulated with a second-order rate constant of $9.1 \times 10^3 \text{ M}^{-1}\text{min}^{-1}$ (black line). The residual [2Fe-2S]²⁺-ISCA1a/2 peak-to-trough CD intensity at 362 and 326 nm at zero time was added on to each data point as there is no evidence for any [2Fe-2S]²⁺ cluster transfer.

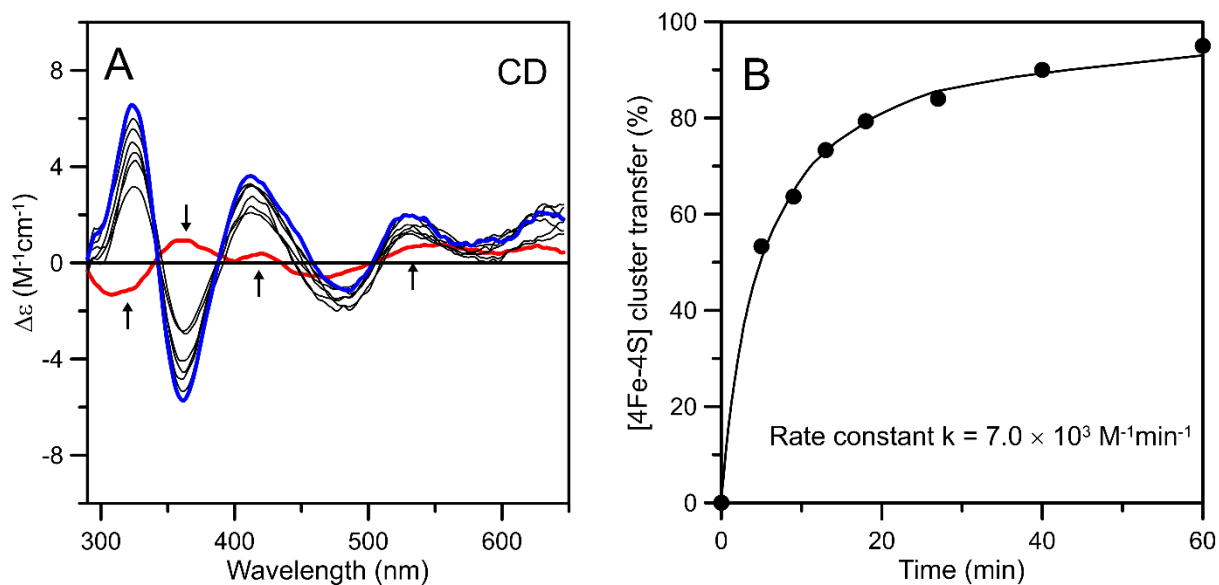


Figure 6. Cluster transfer from *At* [4Fe-4S]²⁺-ISCA1a/2 to *At* apo-NFU5 monitored by CD spectroscopy as a function of time. (A) CD spectra of the cluster transfer reaction mixture that was initially 40 μM in ISCA1a/2 [4Fe-4S]²⁺ clusters and 80 μM in DTT-pretreated apo-NFU5 monomer. The thick red line corresponds to [4Fe-4S]²⁺-ISCA1a/2 recorded before addition of apo-NFU5 to the reaction mixture. The thin grey lines correspond to CD spectra recorded at 5, 9, 13, 18, 27, 40, and 60 min after the addition of apo-NFU5. The thick blue line corresponds to complete [4Fe-4S]²⁺ cluster transfer to NFU5. The arrows indicate the direction of intensity change with increasing time at selected wavelengths and $\Delta\epsilon$ values were calculated based on the initial concentration of [4Fe-4S]²⁺ clusters in the reaction mixture. The cluster transfer reaction was carried out under anaerobic conditions at room temperature in 100 mM Tris-HCl buffer at pH 7.8. (B) Kinetic simulation of cluster transfer from [4Fe-4S]²⁺-ISCA1a/2 to apo-NFU5 based on second-order kinetics and the initial concentrations of [4Fe-4S]²⁺ clusters on [4Fe-4S]²⁺-ISCA1a/2 and of apo-NFU5. Percent cluster transfer was assessed by the difference in CD intensity at 326 and 362 nm (black circles) and simulated with a second-order rate constant of $7.0 \times 10^3 \text{ M}^{-1}\text{min}^{-1}$ (black dots). The residual [2Fe-2S]²⁺-ISCA1a/2 peak-to-trough CD intensity at 362 and 326 nm at zero time was added on to each data point, as there is no evidence for any [2Fe-2S]²⁺ cluster transfer.

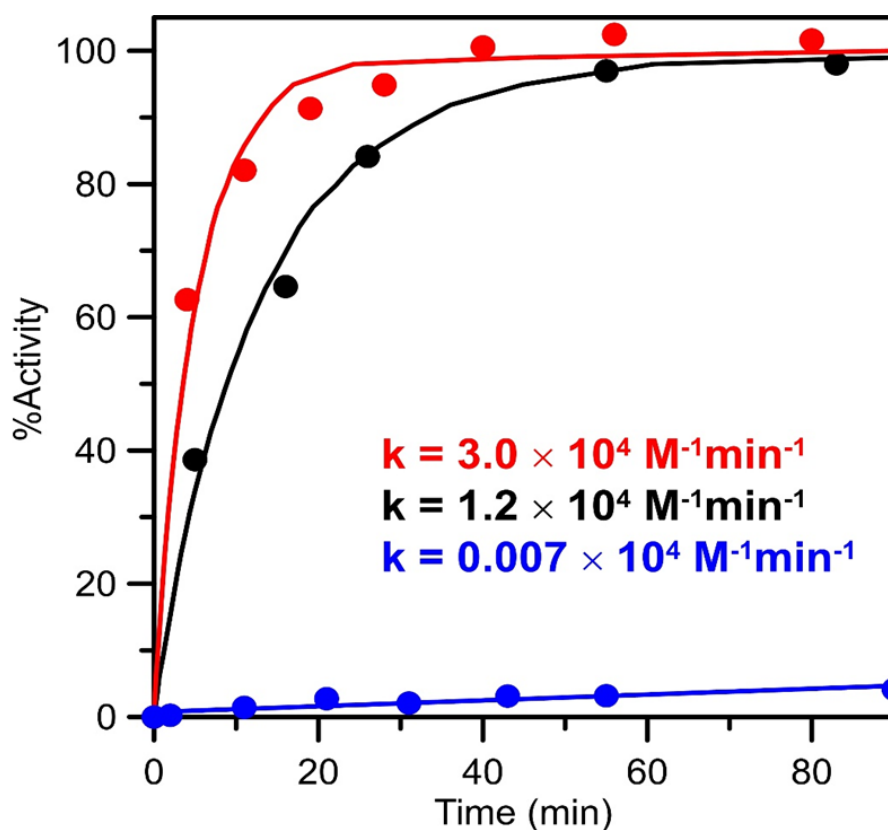


Figure 7. Activation of apo-ACO2 using [4Fe-4S] cluster-bound ISCA1a/2, [4Fe-4S] cluster-bound NFU5, and [2Fe-2S] cluster-bound ISCA1a/2. Apo-ACO2 (2.4 μM) was incubated with [4Fe-4S] cluster loaded ISCA1a/2 (red data) or NFU5 (black data) (both 7.4 μM in [4Fe-4S] clusters) and [2Fe-2S] cluster-loaded ISCA1a/2 (blue data) (14.5 μM in [2Fe-2S]²⁺ clusters) at room temperature under anaerobic conditions. 10 μL aliquots of the reaction mixture were removed at selected time points and assayed immediately for aconitase activity. Residual aconitase activity of apo-ACO2, in the absence of a cluster donor, was assessed and subtracted from all measured activities. Aconitase specific activity as a function of incubation time with the cluster donor was expressed as a percentage of the maximal specific activity of [4Fe-4S]²⁺ cluster-replete ACO2. Solid lines are best fits to second order kinetics, with the indicated rate constants, k , based on the initial concentrations of apo-ACO2 and [4Fe-4S]²⁺ clusters on ISCA1a/2 or NFU5 and half the initial [2Fe-2S]²⁺ cluster concentration of [2Fe-2S]-ISCA1a/2.

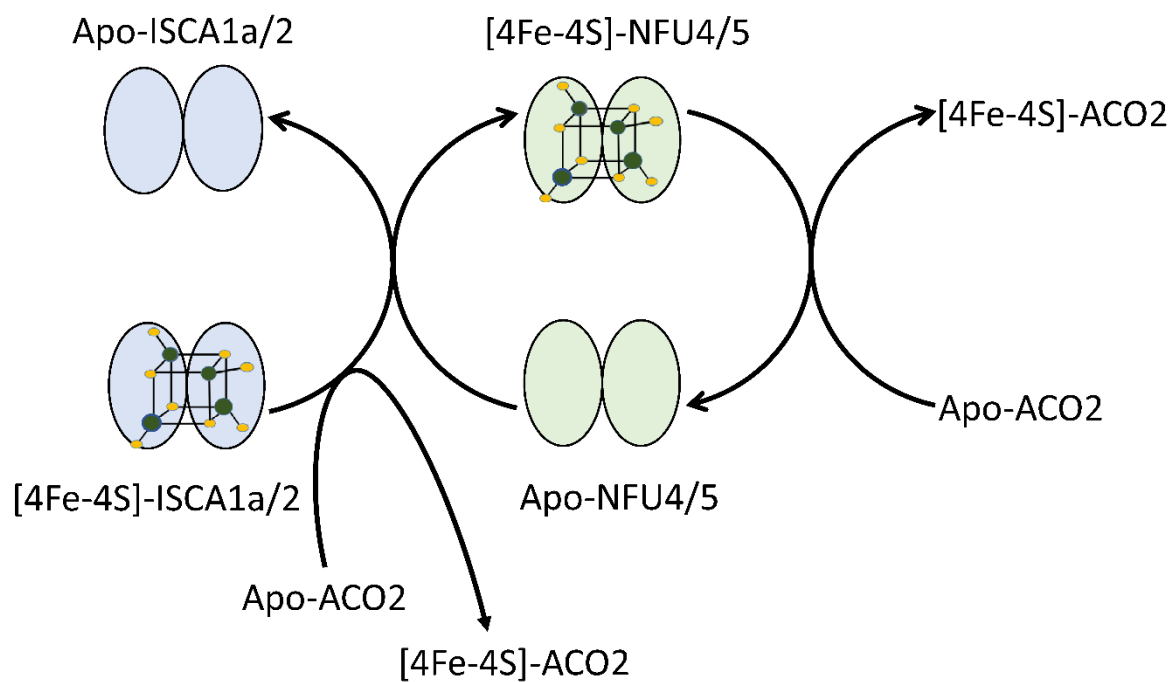


Figure 8. Summary scheme for iron-sulfur cluster trafficking between NFU4 and NFU5 and their partner proteins.

[4Fe-4S] cluster trafficking mediated by Arabidopsis mitochondrial ISCA and NFU proteins

Tamanna Azam, Jonathan Przybyla-Toscano, Florence Vignols, Jérémy Couturier,
Nicolas Rouhier and Michael K. Johnson

J. Biol. Chem. published online October 29, 2020

Access the most updated version of this article at doi: [10.1074/jbc.RA120.015726](https://doi.org/10.1074/jbc.RA120.015726)

Alerts:

- [When this article is cited](#)
- [When a correction for this article is posted](#)

[Click here](#) to choose from all of JBC's e-mail alerts

Supporting information for the manuscript

[4Fe-4S] cluster trafficking mediated by Arabidopsis mitochondrial ISCA and NFU proteins

Tamanna Azam, Jonathan Przybyla-Toscano, Florence Vignols, Jérémy Couturier, Nicolas Rouhier, and Michael K. Johnson

Figure S1. BiFC negative controls verifying that none of the ISCA proteins tested alone with the empty partner vector can restore YFP fluorescence.

Figure S2. Control studies supporting unidirectional [4Fe-4S] cluster transfer from ISCA1a/2 to NFU4 and NFU5.

Table S1. Primers used in this study.

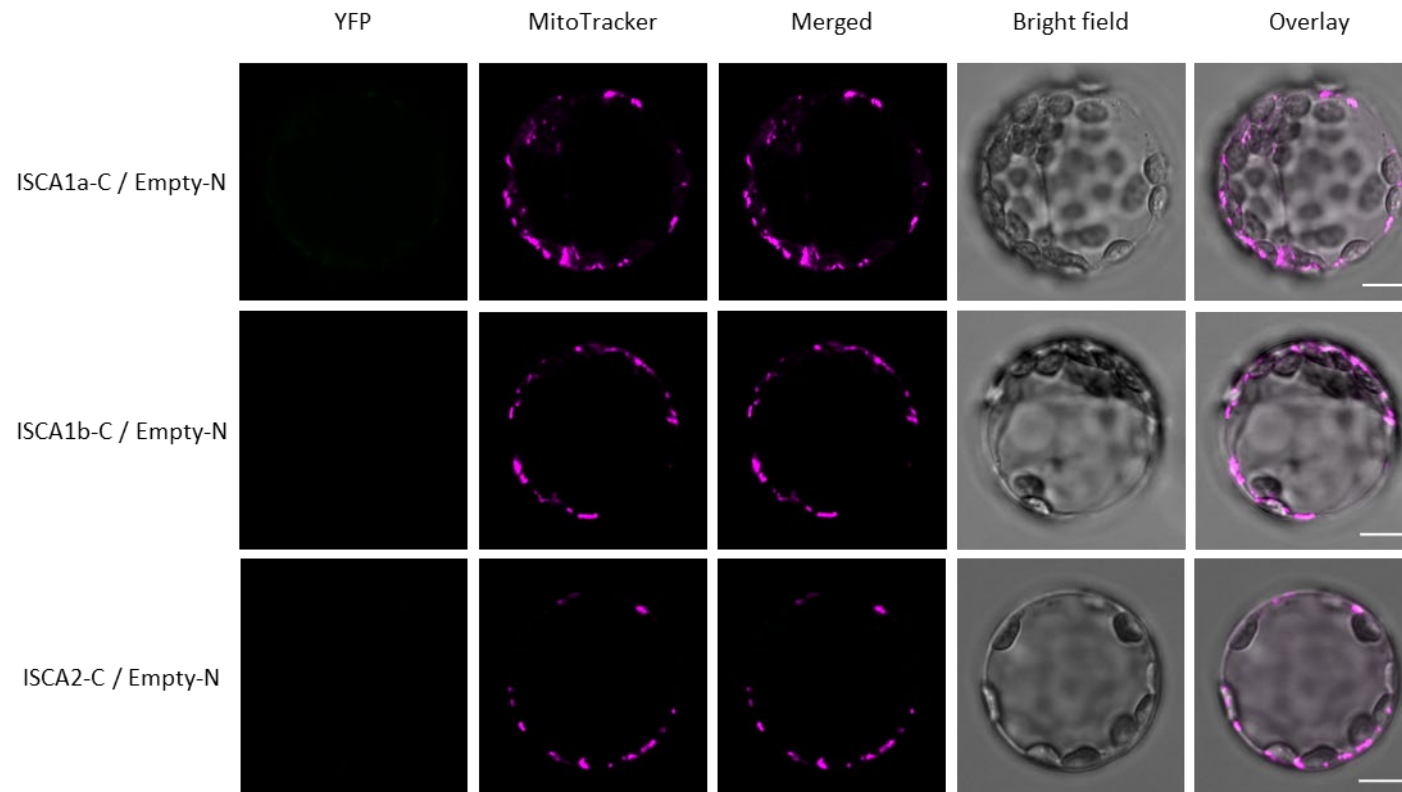


Figure S1. BiFC negative controls verifying that none of the ISCA proteins tested alone with the empty partner vector can restore YFP fluorescence. ISCA-C/empty-N vector pairwise were assayed in Arabidopsis protoplasts isolated from 4 week-old plants in the same conditions as those described for ISCA-C/NFU-N pairwise in Figure 2. Confocal images were captured without Z-stack intensity projection. YFP, yellow fluorescent protein. MitoTracker® Orange CMXRos (Invitrogen) was used at 100 nM to label mitochondria within cells. Bars = 10 μ m.

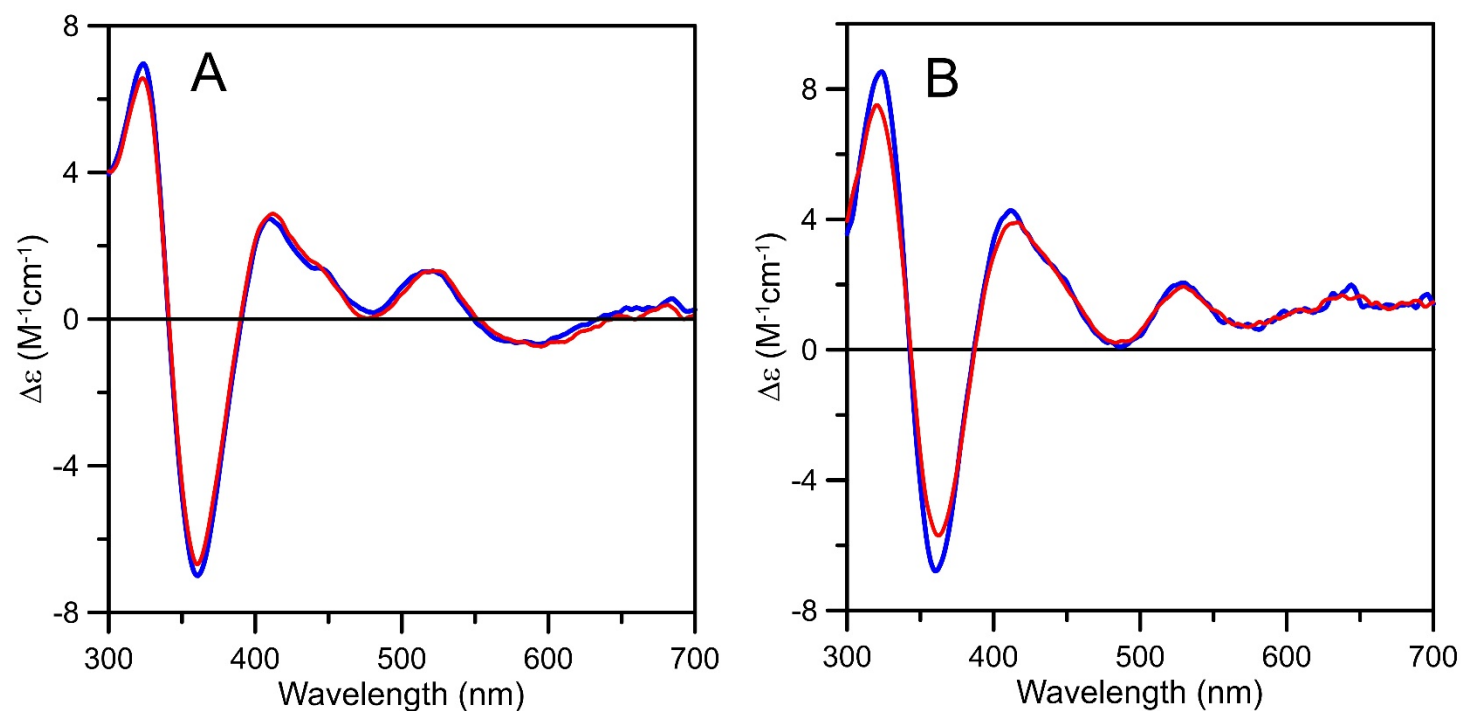


Figure S2. Control studies supporting unidirectional [4Fe-4S] cluster transfer from ISCA1a/2 to NFU4 and NFU5. Attempted [4Fe-4S] cluster transfer from *At* holo-NFU4 (A) and *At* holo-NFU5 (B) to DTT-pretreated *At* apo-ISCA1a/2, monitored by CD spectroscopy as a function of time. CD spectra of the reaction mixture that was initially 50 μM in holo-NFU4 or NFU5 and 80 μM in apo-ISCA1a/2 heterodimers. The blue lines correspond to holo-NFU4 or holo-NFU5 recorded before addition of apo-ISCA1a/2. The red lines correspond to the CD spectra recorded 45 min after the addition of apo-ISCA1a/2. [4Fe-4S] cluster-bound ISCA1a/2 has negligible visible CD, see manuscript text. Consequently, the lack of a significant decrease in the visible CD intensity of [4Fe-4S] cluster-bound NFU4 and NFU5 indicates negligible [4Fe-4S] cluster transfer. The reaction conditions were the same as those used for the successful reverse cluster transfers shown in Figs. 5 and 6.

Table S1. Primers used in this study. Restriction sites required for cloning are in red. For nuclear-encoded plastidial proteins, the sequences coding for the putative targeting sequences have been removed for the cloning in pET and pGADT7/pGBKT7 vectors whereas full-length sequences have been cloned in pUC-SPYNE/SPYCE vectors. Note that a BsmBI type IIs restriction enzyme was used in the ACO2 for primer to generate a compatible NcoI extremity. Primers for cloning GRXS15, BOLA4 in pGADT7/pGBKT7 vectors, are described in (1). The N-terminal domains of NFU4 and NFU5 have been cloned using AtNFU4 for and AtNFU4 rev3 or using AtNFU5 for and AtNFU5 rev3 whereas the C-terminal domains of NFU4 and NFU5 have been cloned using AtNFU4/5 for and AtNFU4 rev or AtNFU5 rev.

Gene names	Plasmids	Primer names	Sequences	N-terminal sequences
NFU4	pET3d, pGADT7, pGBKT7	AtNFU4 for	5' CCCCCATGGCTTTTATCCAAACCCAATCA 3'	MAFIQTQS
		AtNFU4 rev	5' CCCCGGATCCCTACTCTACTCTCATCTC 3'	
	pUC-SPYNE/SPYCE	AtNFU4 for2	5' CCCCTCTAGAATGAAAGGGATTGCGAGG 3'	MKGIAR
		AtNFU4 rev2	5' CCCCTCGAGCTCTACTCTCATCTCTCC 3'	
	pGADT7, pGBKT7	AtNFU4/5 for	5' CCCCCCCCATATGGAGGATGACTCTGAAAC 3'	MEDDSE
		AtNFU4 rev3	5' CCCC GGATCCTTAGCCAGAAGAATAGAAATC 3'	
NFU5	pET3d, pGADT7, pGBKT7	AtNFU5 for	5' CCCCCATGGCTTTTATCCAAACC 3'	MAFIQT
		AtNFU5 rev	5' CCCCGGATCCTCACTCCATTGGACCAGA 3'	
	pUC-SPYNE/SPYCE	AtNFU5 for2	5' CCCCTCTAGAATGAAAGGGCTTACGAGG 3'	MKGLTR
		AtNFU5 rev2	5' CCCCTCGAGCTCCATTGGACCAGAAGA 3'	
	pGADT7, pGBKT7	AtNFU5 rev3	5' CCCC GGATCCTTAACCAGAAGAGTAAAAGTC 3'	
ACO2	pET15b	AtACO2 for	5' CCCCCCGTCTCCATGGCTTCTGAGCATTCTACA 3'	MASEHSY
		AtACO2 rev	5' CCCCTCGAGTTACTTGGCGCTCAAAC 3'	
IBA57.1	pGADT7, pGBKT7	AtIBA57.1 for	5' CCCCCCCCATATGGCGTCTCGCCTTAAATC 3'	MASRLK
		AtIBA57.1 rev	5' CCCCGAATTCCTACGCTGCAGCAACTC 3'	
INDH	pGADT7, pGBKT7	AtINDH for	5' CCCCATATGGCTCTCCGACTACACGGAGTCAAA 3'	MALRLHGVK
		AtINDH rev	5' CCCGGATCCCTATGATGAGTGGCTAGAATG 3'	
ISCA1a	pET28a, pCDFDUET pGADT7, pGBKT7	AtISCA1a for	5' CCCCCCCCATATGAAGCAAGTATTAAC 3'	MKQVLT
		AtISCA1a rev	5' CCCCGGATCCTTAACTAGCACTCTGCTT 3'	
	pUC-SPYNE/SPYCE	AtISCA1a for2	5' CCCCTCTAGAATGAAAGCTTCTCAAATT3'	MKASQI
		AtISCA1a rev2	5' CCCCTCGAGACTAGCACTCTGCTTAGC3'	
ISCA1b	pGADT7, pGBKT7	AtISCA1b for	5' CCCCCCCCATATGCGAAAGCAAGTATTAGCA 3'	MRKQVLA

		AtISCA1b rev	5' CCCC GGATCCT CATGTTGTCGTGAATGACTC 3'	
	pUC-SPYNE/SPYCE	AtISCA1bfor2	5' CCC CTCTAGA ATGAGAAAGCAAGTATTA 3'	MRKQVL
		AtISCA1b rev2	5' CCCC CTCGAGT GTTGTCGTGAATGACTC 3'	
ISCA2	pET12a, pGADT7, pGBKT7	AtISCA2 for	5' CCCCCC CATATG TCCCAACCTGAATCG 3'	MSQPES
		AtISCA2 rev	5' CCCC GGATCCT CAGAGTTTCACCATGAA 3'	
	pCDFDUET	AtISCA2 rev2	5' CCCC CTCGAG GAGTTTCACCATGAAGGA 3'	
	pUC-SPYNE/SPYCE	AtISCA2 for2	5' CCC CTCTAGA ATGTCAAGATCTCTGGTG 3'	MSRSLV
		AtISCA2 rev3	5' CCCC CTCGAG GAGTTTCACCATGAAGGA 3'	

Reference

Couturier, J., Wu, H.-C., Dhalleine, T., Pégeot, H., Sudre, D., Gualberto, J. M., Jacquot, J.-P., Gaymard, F., Vignols, F., and Rouhier, N. (2014) Monothiol glutaredoxin-BolA interactions: Redox control of *Arabidopsis thaliana* BolA2 and SufE1. *Mol. Plant* 7, 187–205